

South China Sea Monsoon Experiment (SCSMEX) and the East Asian Monsoon*

DING Yihui¹(丁一汇), LI Chongyin²(李崇银), HE Jinhai³(何金海), CHEN Longxun⁴(陈隆勋), GAN Zijun⁵(甘子钧), QIAN Yongfu⁶(钱永甫), YAN Junyue¹(阎俊岳), WANG Dongxiao⁵(王东晓), SHI Ping⁵(施平), FANG Wendong⁵(方文东), XU Jianping⁷(许建平), and LI Li⁸(李立)

1 National Climate Center, China Meteorological Administration, Beijing 100081

2 Institute of Atmospheric Physics, Chinese Academy of Sciences, Beijing 100029

3 Nanjing University of Information Science and Technology, Nanjing 210044

4 Chinese Academy of Meteorological Sciences, Beijing 100081

5 South China Sea Institute of Oceanography, Chinese Academy of Sciences, Guangzhou 510301

6 Department of Atmosphere Sciences, Nanjing University, Nanjing 210093

7 The 2nd Institute of Oceanography, State Oceanic Administration, Hangzhou 310012

8 The 3rd Institute of Oceanography, SOA, Xiamen 361005

(Received April 30, 2006)

ABSTRACT

The SCSMEX is a joint atmospheric and oceanic experiment by international efforts, aiming at studying the onset, maintenance, and variability of the South China Sea (SCS) summer monsoon, thus improving the monsoon prediction in Southeast and East Asian regions. The field experiment carried out in May-August 1998 was fully successful, with a large amount of meteorological and oceanographic data acquired that have been used in four dimensional data assimilations by several countries, in order to improve their numerical simulations and prediction. These datasets are also widely used in the follow-up SCS and East Asian monsoon study. The present paper has summarized the main research results obtained by Chinese meteorologists which cover six aspects: (1) onset processes and mechanism of the SCS summer monsoon; (2) development of convection and mesoscale convective systems (MCSs) during the onset phase and their interaction with large-scale circulation; (3) low-frequency oscillation and teleconnection effect; (4) measurements of surface fluxes over the SCS and their relationship with the monsoon activity; (5) oceanic thermodynamic structures, circulation, and mesoscale eddies in the SCS during the summer monsoon and their relationship with ENSO events; and (6) numerical simulations of the SCS and East Asian monsoon.

Key words: East Asian monsoon, South China Sea monsoon experiment (SCSMEX), monsoon onset, low-frequency oscillation

1. Introduction

It has been over 70 years by far for the study on the monsoon over China since as early as the 1930s (Zhu, 1934). For a long time, the Chinese meteorologists have made great efforts in the exploration and prediction of the East Asian monsoon and have achieved quite a few significant results, which have profound influences at home and abroad (Tao and Chen, 1987; Chen et al., 1991; Ding and Murakami, 1994; Ding, 1994; Zhu et al., 1990). The scientific results about the East Asian summer monsoon research

before the South China Sea monsoon experiment (SCSMEX) can be summarized in six aspects (Ding and Ma, 1996): (1) revealed the abrupt change of the Asian monsoon and the circulation over East Asia (Yeh et al., 1958); (2) found the existence of the East Asian monsoon system, which is driven by a heat source over the South China Sea (SCS) -West Pacific, while a cold source over Australia (Tao and Chen, 1987); (3) disclosed that the earliest summer monsoon onset, on average in mid-May, is around the SCS in the seasonal march of the Asian monsoon (Tao and Chen, 1987); (4) pointed out that the intra-seasonal low-frequency

*Supported by the National Key Program: SCSMEX under Grant 98-monsoon-7-3.

oscillation is closely related to the medium-range variation of the East Asian monsoon circulation and the precipitation (Wang and Ding, 1992). The meridional propagation of low-frequency oscillation plays a significant role in the droughts and flooding events over China, especially over the Yangtze-Huaihe Basin (Ding, 1993); (5) revealed the affinities among the activities of the East Asian monsoon and the seasonal march of the main rain belts over the East-Asian and their relation with droughts and flooding events. The main rain belt over China advances in a step way of two abrupt northward jumps and three stationary stages (Guo and Wang, 1981; Ding, 1992). All the circulation situations of persistent and intensive rainfall events are closely related to the abnormal activities of the East Asian monsoon; and (6) noted the prominent relationship among the ENSO events, the convective activities over the warm pool, the East Asian monsoon, and the related precipitation (Huang and Li, 1988; Nitta, 1987).

As is widely concerned, the SCS is the region where the Asian summer monsoon breaks out the earliest. After the SCS monsoon onset, it expands northward and northeastward over East Asia. On the other hand, it advances to the Bay of Bengal (BOB) and the Indian Subcontinent, which leads to the Indian summer monsoon onset in the first decade of June. Although the onset facts and the large-scale synoptic processes are recognized to some extent before the SCSMEX, further knowledge about the synoptic and dynamic processes of the onset is insufficient and there is no consistent viewpoint with regard to the onset mechanisms[†]. And many researchers have put forward various hypotheses. It is also obscure concerning the interaction between the SCS and the onset, maintenance of the summer monsoon. Therefore, it is necessary to study the physical processes and mechanisms from the perspective of land-sea-atmosphere coupling systems. On the other hand, more than 10 years have elapsed since the international monsoon experiment (MONEX) carried out in 1978-1979, during which tremendous progress had been made in radar,

satellite, and oceanic observation so that it is likely to obtain more perfect and accurate multi-scale land-sea observational data. In addition, due to the development and application of various advanced global and regional models, many necessary conditions are available for the assimilation, simulation, and prediction of the weather and climate. These scientific thoughts and technical development mentioned above shaped the scientific motivation and basis of carrying out a new MONEX in the SCS and its vicinities.

The SCSMEX is aimed to better understand the mechanism of the onset, maintenance, and variability of the summer monsoon over the SCS and ultimately improve the monsoon prediction. To attain this goal of SCSMEX, the following four specific scientific objectives were set: (1) to describe and document the space-time evolution of the large-scale atmospheric circulation, thermodynamic fields, as well as basic ocean flow patterns and thermohaline structures associated with the SCS monsoon; (2) to identify the influence of heating contrasts between SCS and surrounding regions and the role of early monsoon (April-May) convection and multi-scale processes in the SCS in the abrupt transition and subsequent evolution of the East Asian monsoon; (3) to elucidate physical processes in oceanic response to monsoon forcing and air-sea interaction in SCS and relationships with adjacent oceans; and (4) to assess and improve the ability of regional and global models in simulation and prediction of the monsoon onset in Southeast Asia and South China.

The SCSMEX is a large-scale joint atmospheric and oceanic field experiment. It is an international effort with many participating countries and regions cooperatively involved in this experiment and the subsequent research work, including 10 provinces of China, Taiwan, Hongkong, Macao, USA, Australia, Japan, Thailand, Vietnam, Malaysia, Singapore, Brunet, Indonesia, Philippine, etc.

2. Field observations and data acquisition

The field observation phase that covered the period from 1 May to 31 August 1998 is one of the core

[†]SCSMEX Office, 1995 South China Sea Monsoon Experiment (SCSMEX).

components of SCSMEX. The observation field was divided into a large-scale observation region and an intensive observation domain. The former included a large Asia-West Pacific region (10°S - 40°N , 70° - 150°E), with the focus on conventional observations. The latter was located on the SCS and its surrounding regions (10°S - 30°N , 95° - 130°E) (see Fig.1). Field observations consisted of an atmospheric observation network, an oceanographic observation network, an air-sea interface observation network, and a satellite observation network. The observation system consisted of the most advanced atmospheric and oceanic observation platforms and instruments including radiosonde (conventional and GPS type), surface observation network, weather radar, a scientific research ship, aerosondes, satellite observation (polar, geostationary, and TRMM satellites), oceanic boundary layer and air-sea interface flux measurement, integrated sounding system (ISS), wind profiler, radiation, ATLAS moorings, drifting buoys, acoustic Doppler current profile (ADCP), towed profiling (CTD) and airborne expendable bathythermographs (AXBT),

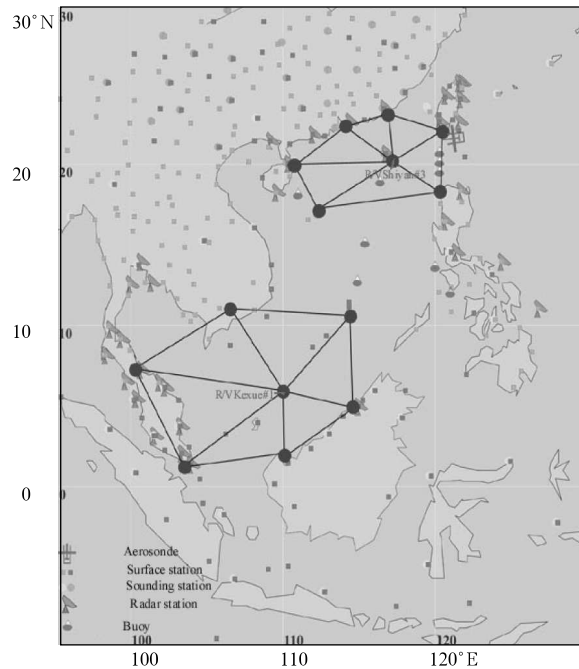


Fig.1. The SCSMEX observation network for the field experiment of May-August 1998 (intensive observation period (IOP)).

and so on. Two mesoscale observation networks were nested in the intensive observation domain. One mesoscale flux measurement network (Fig.2) which comprised a dual-Doppler array was particularly designed for the observation of convection and mesoscale convective systems over the northern SCS.

There were two intensive observation periods (IOPs) during the field observation (5-25 May and 5-25 June). The first IOP focused on monitoring the onset of the SCS monsoon and its sudden seasonal change as well as the implications for precipitation in South China and Southeast Asia. The second IOP focused on monitoring the atmospheric and oceanic conditions over SCS during the period of the mature phase and northward migration of the East Asian monsoon, and the implication for precipitation in the Yangtze River Basin, the Korean Peninsula, and Japan. A wealth of information and data were obtained during the periods of monsoon onset over SCS and the northward migration of the East Asian monsoon, which provided necessary basis for further researches. A comprehensive and complete database of the SCSMEX had been

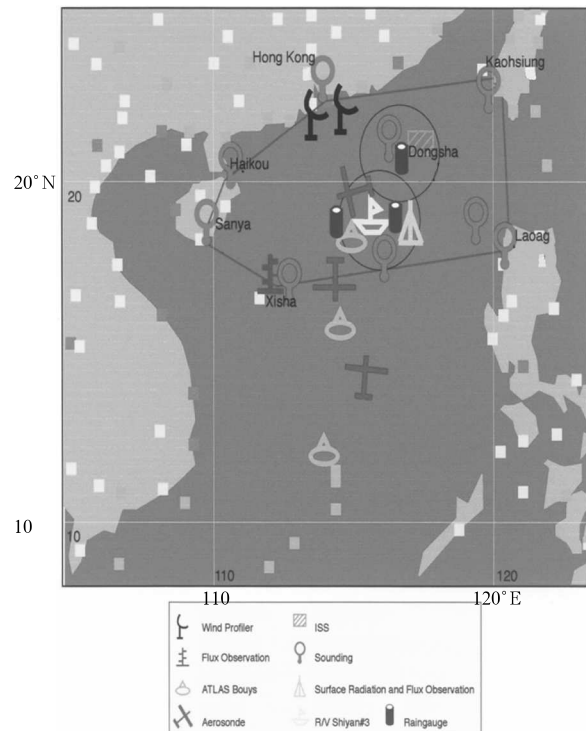


Fig.2. Observing array for the northern SCS during the IOP of SCSMEX.

set up after April 2001, which met the international standard and included all kinds of meteorological observations, special observations, oceanographic observations, radar and satellite data, four-dimensional limited area assimilation data, TBB, precipitation data, etc. The data obtained from the field observation have been widely used in four-dimensional data assimilation, numerical weather forecast experiment, and monsoon research by China, Japan, USA, and other countries (Ding and Li, 1999; Lau et al., 2000). The primary research achievements of the SCSMEX will be presented in the following sections.

3. Onset of the SCS summer monsoon

One of the most significant features in the seasonal march of the East Asian summer monsoon is the sudden onset of summer monsoon over the SCS around mid-May, which marks the arrival of the East and Southeast Asian summer monsoon and the commencement of the rainy season. This abruptness has never been seen in other Asian monsoon areas (Lau and Yang, 1997). It can be seen from Fig.3a that this process of the SCS summer monsoon onset is accomplished in quite a short time period. In contrast, over the Indian longitudes this onset process is more or less gradual though a large increase in rainfall amount in this region may be noted (Fig.3b). This suddenness of the onset process of the SCS monsoon occurred in the 4th pentad (16-20 May) has been well docu-

mented by numerous investigators based on various monsoon index or parameters (Qian and Lee, 2000; He et al., 2001), thus identifying the SCS summer monsoon onset in the mid-May, while it withdraws out of the SCS at the beginning of November. Many investigators discussed the difference of large-scale circulation over the Asian monsoon region before and after the onset of the SCS summer monsoon based on large-scale wind, geopotential height, and OLR distributions (Matsumoto, 1997; Fong and Wan, 2001; Wang and Lin, 2002). It can be seen from Figs.4 and 5 that these physical fields have undergone significant changes in the third (11-15) to fourth (16-20) pentads of May, with the southwesterly wind rapidly expanding from the equatorial East Indian Ocean region to the Indo-China Peninsula and then down to the most part of the SCS (Figs.4a, b). Twin cyclone over the equatorial Indian Ocean region can be constantly observed across the equator. Meanwhile, the OLR decreases from 240 W m^{-2} to less than 230 W m^{-2} (Fig.5) in the short transition period, indicating the sudden development of convection and rainfall amount over SCS during the onset period. Concerning the difference of the 850 hPa wind pattern (Fig.5e) between the 2nd pentad (6-10 May, before the onset) and the 5th pentad (21-25 May, after the onset) and the corresponding difference of the OLR field (Fig.6e), much attention should be paid to the most dramatic change of the low-level wind pattern: the acceleration and eastward extension of the

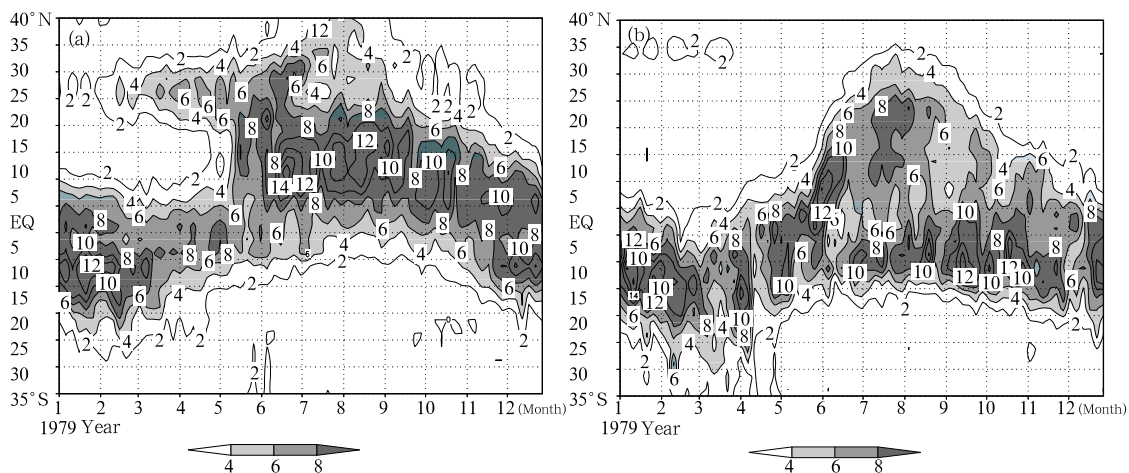


Fig.3. Latitude-time cross-sections along 110° - 120° E (a) and 70° - 80° E (b) averaged for 1979-2001 based on CMAP data.

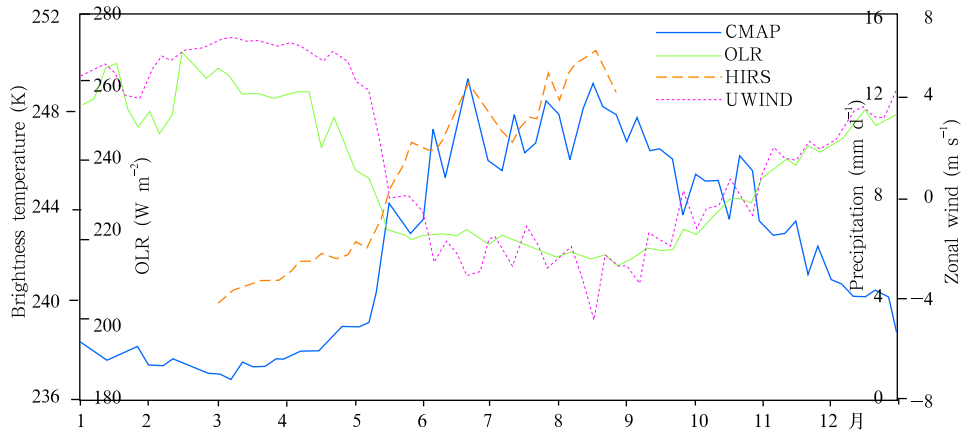


Fig.4. Monthly variation of CMAP precipitation (mm d^{-1}), brightness temperature (K), OLR (W m^{-2}), and 850-hPa zonal wind (m s^{-1}) in the region of 10° - 20° N, 110° - 120° E averaged for 1980-1995 (Qian and Lee, 2000).

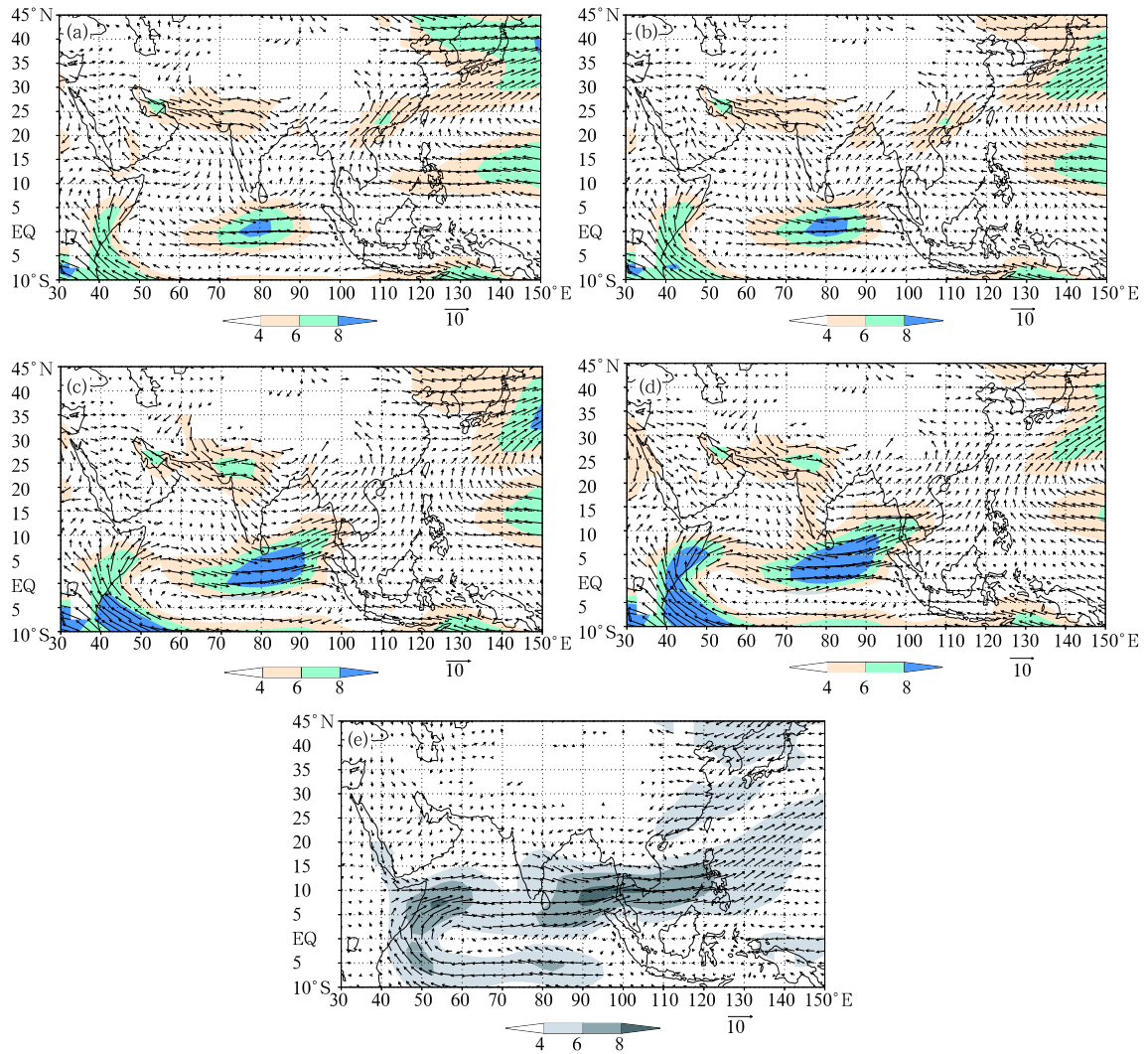


Fig.5. Mean 850-hPa wind field averaged for 1979-1999. (a) For the 2nd pentad of May (6-10), (b) the 3rd pentad of May (11-15), (c) the 4th pentad (16-20), (d) the 5th pentad (21-25), and (e) the difference between the 5th and the 2nd wind fields (unit: m s^{-1}). Shaded areas denote the regions with wind speed greater than 8 m s^{-1} .

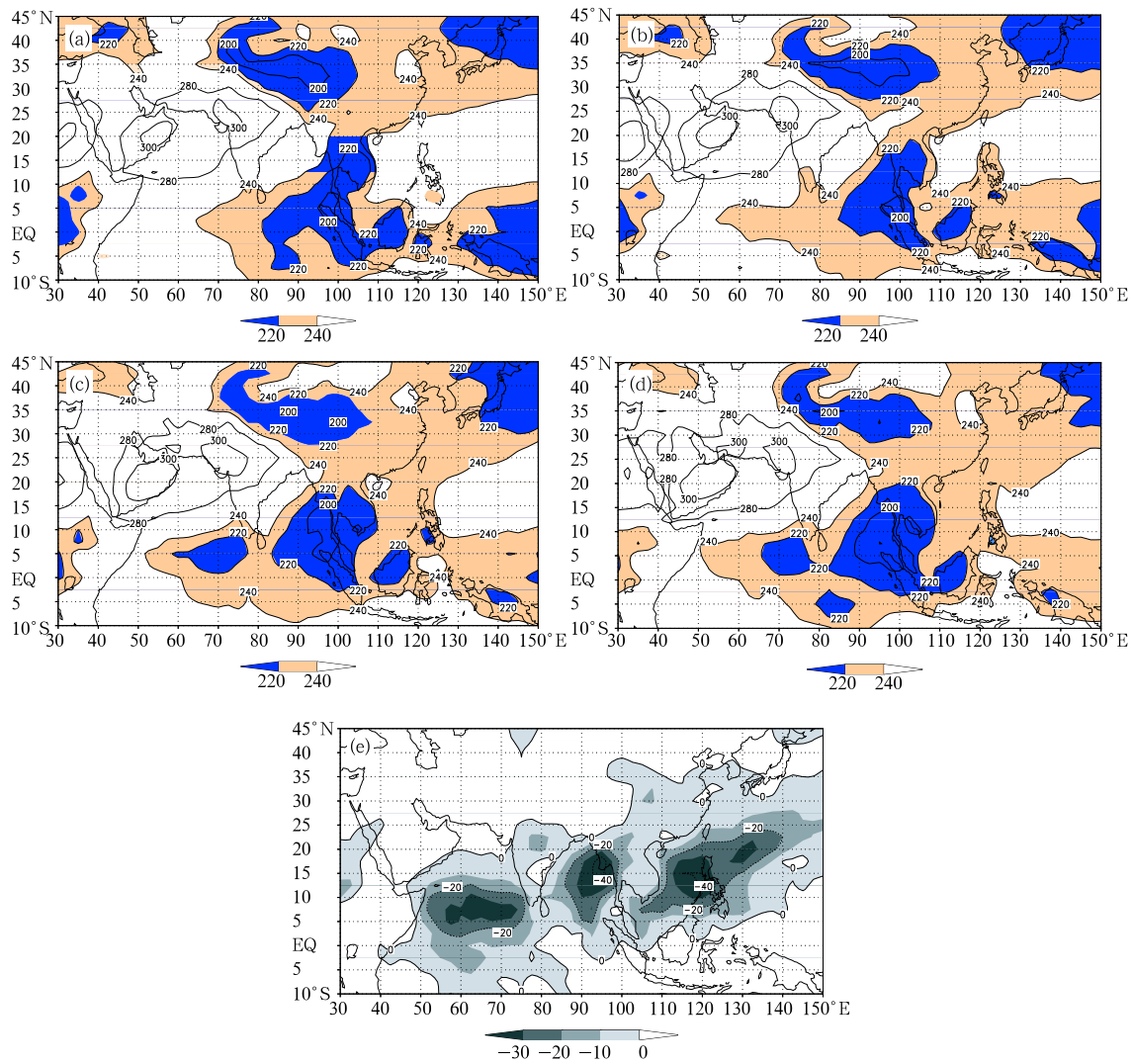


Fig.6. As in Fig.5, but for OLR field (unit: $W m^{-2}$). The regions of $OLR < 240 W m^{-2}$ are shaded.

tropical westerly wind from the tropical East Indian Ocean to the central and southern SCS, the remarkable intensification of the upstream Somali jet and the occurrence of a shear line embedded with two cyclonic circulations from the BOB to the northern SCS which corresponds to the monsoon troughs. Therefore, the onset of the summer monsoon in the SCS should be considered as a regional demonstration of the rapid seasonal intensification of the whole Asian summer monsoon. Correspondingly, the most significant change in the OLR pattern is also seen in the Arabian Sea, the tropical East Indian Ocean, the BOB, the SCS, and the tropical West Pacific. These changes reflect abrupt enhancement of cloud and rainfall in

these regions. Among them, the change in the SCS is the most marked. Another sudden change is the rapid weakening and eastward retreat of the subtropical high over the West Pacific from the Indo-China Peninsula and the SCS (figure omitted). At the same time, a trough over the BOB continuously extends southward and deepens. However, it is not clear which one, eastward extension of low-level southwesterlies or the eastward retreat of the subtropical high, is the primary cause for leading to large-scale abrupt changes in the above chain of events. Fong and Wang (2001) pointed out that the establishment of the SCS summer monsoon during the fourth pentad of May is only confined to the lower troposphere, with a ridge of

the subtropical high and upper-level southeasterlies or northeasterlies still dominating the SCS, showing that the main body of the subtropical high has not significantly changed. Therefore, they concluded that the onset of the low-level monsoon in the SCS initially forces the subtropical high to move eastward, whereas the feedback process of convective and mesoscale activities over the Indo-China Peninsula and the SCS possibly makes an important contribution to the final withdrawal out of the SCS of the subtropical high at a later stage. Intensive vertical transports of heat produced by vigorous convective activity may significantly heat the upper troposphere and induce high-level outflow, thus leading to decrease of pressure at low-level or the development of a trough. This is associated with the breaking of the continuous subtropical high belt in the Northern Hemisphere around the region of the BOB when the pre-monsoon begins in late April or early May. This kind of feedback mechanism should be further studied with numerical simulation and theoretical analysis.

The most salient feature of the 200-hPa wind patterns is the significant development and northward movement of the South Asian high over the eastern part of the Indo-China Peninsula. Before the onset of the SCS monsoon, the South Asian high is located in the southern part of the Indo-China Peninsula, and has a weaker intensity (figure omitted). Thereafter, this high moves toward the northwest and significantly intensifies. The upper-level westerly jet and the easterly jet on either flank of the high accelerate, thus leading to the intensification of 200-hPa divergence and convective activity. Before the onset, the major divergence center rapidly moves over the central and southern part of the SCS, with marked divergent airflow found in these regions. This pattern of upper level divergence lends some support to the idea of a feedback mechanism driven by enhanced convective activity. From the heating pattern (figure omitted), it can be seen that this major outflow region corresponds to the extensive area of the heat source ($Q_1 > 0$) in these regions.

Based on the above analysis, the chain of significant events during the onset of the SCS summer mon-

soon may be identified as follows: the development of a cross-equatorial current in the equatorial East Indian Ocean (80° - 90° E) and off the Somali coast, and the rapid seasonal enhancement of heat sources over the Indo-China Peninsula, South China, the Tibetan Plateau, and neighboring areas; the acceleration of low-level westerly in the tropical East Indian Ocean; the breaking of the continuous subtropical high belt around the BOB and the development of a monsoon depression or cyclonic circulation; the eastward expansion of tropical southwest monsoon from the tropical East Indian Ocean; the arrival of the rainy season in the regions of BOB and Indo-China Peninsula and the impacts from mid-latitudes; further eastward expansion of the southwesterly monsoon into the SCS region; the significant weakening and eastward retreat of the main body of the subtropical high, and eventual onset of the SCS summer monsoon with convective clouds, rainfall, low-level southwesterly wind and upper-level northeasterly wind suddenly developing in this region.

The climatological and case study in 1998 made by He et al. (2000, 2003) supported the above evidence on the onset process. They pointed out that with the rapid movement of the South Asian high from the east to the Philippines (April) to the northern Indo-China Peninsula, the BOB trough deepens and strengthens. The partial westerly wind at the trough bottom converges with the tropical westerly coming from the Southern Hemisphere, which forms strong westerlies over the tropical Indian Ocean and then flows to the Indo-China Peninsula. As can be seen from Fig.7a, about 15 days before the onset of the SCS summer monsoon, the westerly over the equatorial Indian Ocean (EQ, 80° E) not only increases steadily but also extends and propagates northeastward, accompanied by a northeastward moving low OLR area (Fig.7b). When the westerly wind spreads to the SCS area (15° N, 110° E), the SCS summer monsoon establishes. Corresponding to the abrupt change of the large-scale circulation, the meridional temperature difference between the low and middle latitudes of Asia and the zonal wind shear of lower latitudes also change distinctively. On the average, the sign of the meridional temperature difference of the low and

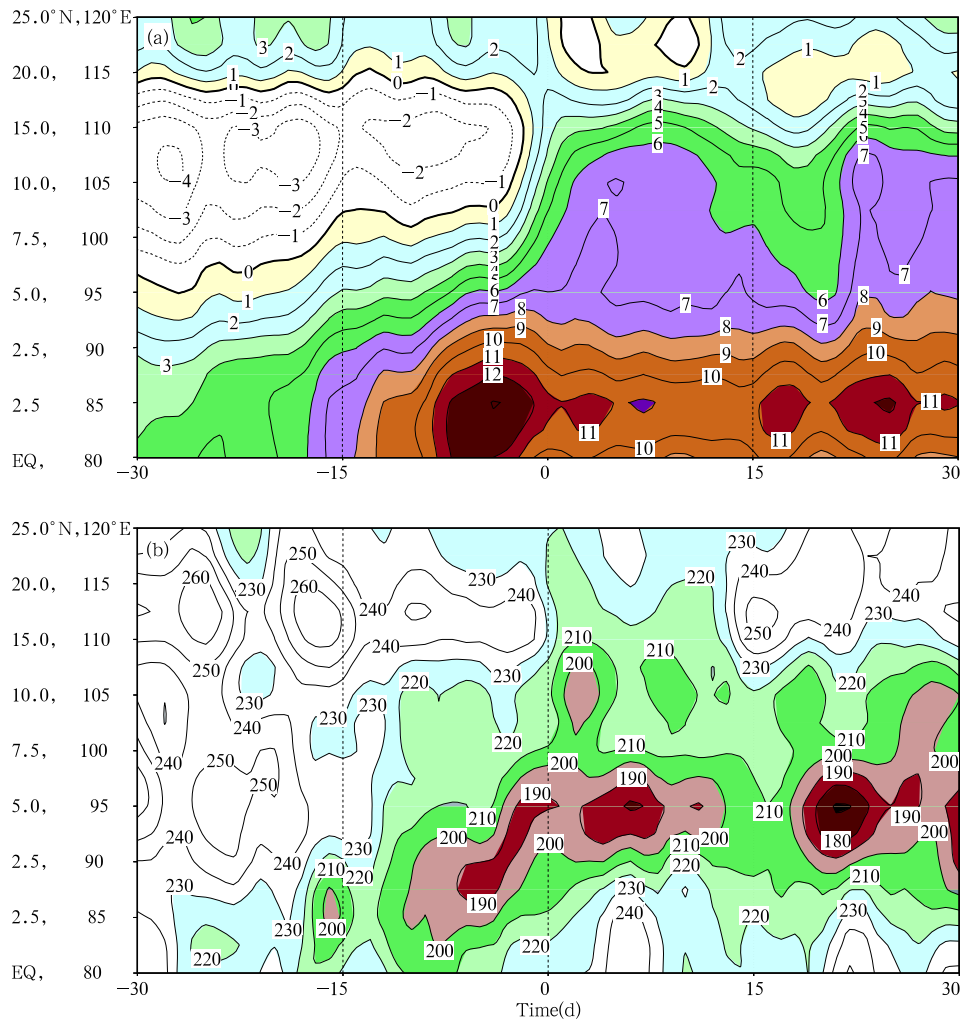


Fig.7. Longitude-time (from (EQ, 80°E) to (25°N, 120°E)) cross-section for 850-hPa zonal wind (a) and OLR (b) around the onset of the SCS summer monsoon composited for 1990-1998. The shaded areas in (a) are westerly wind regions. The shaded areas in (b) are regions with $OLR < 230 W m^{-2}$ (He et al., 2000).

middle latitudes east to 90°E changes stably in the middle and late May, and it firstly takes place in the Indo-China Peninsula area, while it occurs in early and middle June in the western BOB and Indian region. The date on which the sign of the zonal wind shear change is slightly earlier than that of the meridional temperature difference, and it shows a west-earlier-east-later feature, which may be associated with the eastward spread of the equatorial westerly and the southwesterly in the front of the strengthened BOB trough.

Fong and Wang (2001) clearly illustrated the process of the eastward expanding and acceleration of the tropical southwesterly from the tropical East Indian

Ocean (figure omitted). In April and early May, the low-level southwesterly develops slowly in the near-equatorial East Indian Ocean where the strongest low-level westerly can be observed. In this period, the Somali jet along the East African coast initially forms with relatively strong wind speed observed only to the south of the equator. The early development of the near-equatorial strong westerly in the equatorial East Indian Ocean can be found in the longitudinal range of 80°-90°E (Matsumoto and Murakami, 2002). Westerly wind rapidly propagates eastward from the 27th to 28th pentads. On the one hand, it crosses the Indo-China Peninsula and reaches the most parts of the SCS, and on the other hand it extends upward from

nearly 700 hPa up to 400 hPa. It suggests from the above evolution that the onset of the SCS summer monsoon be mainly the consequence of the explosive development and eastward expansion of the southwest-erly in the tropical East Indian Ocean. It is a regional demonstration of the sudden variation of the basic cur-rent with the seasonal transition.

Following the sequence of the SCS summer monsoon onset dates from 1953 to 1999, Yan (1997) fur-ther classified the SCS summer monsoon onset into three types: the first one is the earliest onset over the northern SCS, and then outbreaks in the whole SCS area, with a frequency of 27.6%; the second one is over the southern SCS, then expands northward gradually, 15%; and the third one is simultaneous onset through-out the SCS area, 57.4%. The SCS monsoon onset in 1998 belongs to the first type (Lau et al., 2000; Ding and Liu, 2001). The onset process of the SCS summer monsoon began with the development of a twin cyclone around the oceanic region near Sri Lanka. Firstly there is a twin cyclone straddling the equator forming near Sri Lanka. In between, the equatorial westerly appeared over the equatorial Indian Ocean in the second pentad of May and accelerated, the SCS re-gion was controlled by the easterly to the south of the the subtropical high over the West Pacific. In the third pentad of May, the Sri Lanka depression moved east-ward and northward and the equatorial Indian west-erly further accelerated, but their effect did not reach the Indo-China Peninsula at this time. Over most of the SCS and central part of the Indo-China Peninsula, the easterly at low and middle levels prevailed due to dominance of the subtropical high in those regions, the westerly were only observed in South China and the northern Indo-China Peninsula. In the fourth pen-tad of May, the tropical southwesterly to the west of the subtropical high and equatorial East Indian Ocean westerly started to accelerate and dominated over the northern part of the SCS, the subtropical high over the West Pacific moved northeastward rapidly. It can be found that this process of eastward propagation of the tropical monsoon occurred nearly at the same time as the eastward withdraw of the subtropical high and significant southward intrusion of cold air from mid-

latitude into South China and the northern SCS. The fifth pentad of the May, the subtropical high with-draw out of SCS completely, strong low level tropical westerly dominates the BOB, Indo-China Peninsula, and throughout the SCS, which denotes the full es-tablishment of the SCS summer monsoon. He et al. (2000) further noted that the precipitation zone moved northeastward as well as the southwesterly at low level expanded eastward.

Finally, the climatological onset dates of the Asian summer monsoon in different regions are sum-marized on the basis of various studies. The Asian summer monsoon breaks out and advances at four stages: (1) The earliest onset is often observed in the south of the western Indo-China Peninsula in late April and early May (Lau and Yang, 1997; Mat-sumoto, 1997; Webster et al., 1998; Wang and Fan, 1999). And some investigators have argued that the Asian summer monsoon may occur firstly in BOB-Myanmar (Wu and Zhang, 1998) or the central SCS (Chen Longxun et al., 2000). Therefore, the earliest onset of the Asian summer monsoon may be over an extensive areas around the Indo-China Peninsula and is most often in the central Indo-China Peninsula. In addition, mid-latitude circulations affect rainfalls at this stage. (2) The summer monsoon prevails in ex-tensive regimes at this stage and advances northward up to the BOB while eastward up to the SCS. The advance of the summer monsoon is usually abrupt or rapid and most often occurs during the period from mid to late May. The summer monsoon over the SCS just breaks out at this stage. And numerous investiga-tors have illustrated the major features of circulations and rainfalls of this stage (Chan et al., 2000), which are in good correspondence with what are observed at the first stage of the three individual stages of the on-set of the Asian summer monsoon pointed out by Wu and Wang (2001) that the rainfall rate increases sig-nificantly, the height at 500 hPa decreases due to the sudden northeastward retreat of the subtropical high over the West Pacific, the zonal winds at 850 hPa in areas from the BOB to the SCS strengthens along 5°-10°N, the anticyclonic wind fields over the Tibetan Plateau develops, the upper-level divergence increases

and the deep convection strengthens suddenly. During this stage (the first dekad of June), the pre-summer rainy season in SCS (also including the Meiyu in Taiwan) reaches its peak. (3) This stage is well known for the onset of the Indian summer monsoon and the arrival of the East Asian rainy seasons such as the Meiyu over the Yangtze River Basin and the Baiu season in Japan. These significant events usually occur during the period from the first dekad to the second dekad of June (Ding, 1992; Chen et al., 1991; Ding and Murakami, 1994; Oh et al., 1997). The earlier onsets of Changma in southern Korean Peninsula may be observed in the third dekad of June for some years. And (4) the summer monsoon at this stage advances up to North China, the Korean Peninsula, and even North Japan in the first or second dekad of July (Oh et al., 1997; Tanaka, 1992). Starting from the second half of July, the rainy season in Northeast China begins with the summer monsoon prevailing in this region. This is the northmost position of the Asian summer monsoon reaching.

Four major viewpoints on the mechanisms of the onset of SCS summer monsoon before SCSMEX are as follows: (1) the influence of SST; (2) the tropical forcing, which mainly indicates the intraseasonal low frequency oscillation under the background of the seasonal change of the general circulation as well as the large-scale seasonal shift of pressure gradient (from winter to summer) due to the thermal difference between Asia and Australia; (3) the triggering mechanism of mid-latitude systems; and (4) the thermal contrast between Asia and its surrounding oceanic areas. Especially, the Tibetan Plateau as a major heat source plays an important role in forming this thermal contrast. These mechanisms are better understood through the studies in recent years and it is confirmed that the seasonal shift from winter to summer and the corresponding seasonal evolution of the tropical large-scale circulation and thermodynamics determine the general onset process and even the direction of the onset advance of the summer monsoon. Under the large-scale background established by the seasonal evolution, the arrival of several wet phases of ISO propagating one-after-another can trigger the development

of deep convections. Because of the seasonal regulation, the ISO has a tendency to be phase-locked at fixed periods and locations, and then causes the onset of the monsoon (Wu and Wang, 2001). In the above mentioned mechanisms of monsoon onset, the seasonal evolution of sea-land thermal contrast is a precondition, the SST and the Tibetan Plateau heat sources are regional factors that directly bring about the onset or its enhance, and the mid-latitude oscillation, the tropical synoptic systems, and the low frequent oscillation are important triggering factors.

The SST over the eastern equatorial Pacific has a significant impact on the timing of the onset dates of summer monsoon over the SCS. Chen et al. (1999), Xie et al. (1999), and Chen Yongli et al. (2000) indicated that in El Niño/La Nina year (or SSTA is positive/negative in the eastern equatorial Pacific), the SCS summer monsoon onset is usually later/earlier than normal. This may be caused by a stronger/weaker western Pacific subtropical high located at an anomalous position farther south and west/north and east than its normal location due to the anomalous Walker cell. Moreover, the preceding winter general circulation may also influence the timing of the onset of the following the SCS summer monsoon through the SST of the western Pacific Ocean, in that during the strong winter monsoon years, the northward movement of the Kuroshio Current is suppressed, thus the SST over the west part of the West Pacific is colder than normal in spring, and then the onset of the SCS summer monsoon is affected. In addition, the SST of the SCS at the prophase of the onset greatly affects the timing of the onset as a local mechanism and the positive SSTA is generally believed advantageous to the onset. Zhu and Xu (2000) found that the SST of the SCS in 1998 showed the 30-60-day low frequency oscillations. And at the onset stage of the monsoon, phases of the low frequency oscillation of rainfalls lagged behind those of the SST for about six days, and the low frequency oscillation of the SST of the SCS played a triggering role in the onset of its summer monsoon. Chen and Wang (1998) and Liu and Chen (1999) simulated the timing of the onset of summer monsoon over the SCS using the CCM3, NCAR, GCM model, adding

in a forcing of $\pm 1^{\circ}\text{C}$ of SST individually in the SCS, the warm pool of the western Pacific Ocean, the eastern equatorial Pacific Ocean, BOB, and the Southern Hemispheric ocean areas and integrating from April to September. It can be found that $\pm 1^{\circ}\text{C}$ of the SST in the SCS and $\mp 1^{\circ}\text{C}$ of the SST in the Southern Hemispheric ocean areas to the south of the SCS are favorable for the early/late SCS summer monsoon onset and the earliest/latest onset occurs when the SST of the SCS is 1°C warmer/colder while the SST of the Southern Hemisphere is 1°C colder/warmer than normal.

Many investigators (Chen and Zhu, 1998; Mu and Li, 2000; Li and Wu, 2000; Chen et al., 2001) have revealed the relationship between the low frequency oscillation and the SCS summer monsoon onset in 1998 and it is accordantly believed that the SCS summer monsoon onset at 850 hPa is related to the first formation of the low frequency cyclonic band over the SCS in May. This cyclonic band emerged over the western Pacific Ocean on 10 May (Fig.8 C1) and expanded westward to the oceanic areas to east of Taiwan and Philippine on 15 May, and eventually reached the SCS on 20 May when the summer monsoon over the SCS broke out. Then, a low frequency anticyclonic zone developed to the south of the low frequency cyclonic band (Fig.8 A1) and moved westward from West Pacific into the SCS on 9 June. The low frequency cyclonic band C1 began to shift northward into the main land on 4 June, then to south of the Yangtze River on 9 June and arrived at the middle and lower reaches of the Yangtze River on 14 June when Meiyu started over this region. The above mentioned facts reveal that the low frequency oscillation associated with the onset of the SCS summer monsoon in some years (such as 1980, 1988, and 1998) forms over the western Pacific Ocean and travels westward to the SCS, exerting an important triggering impact on the onset of SCS summer monsoon.

The thermal effect of the Tibetan Plateau is also one of the mechanisms that influence the onset of the SCS summer monsoon. So far, it has not been still clear why the thermal effect of the Tibetan Plateau firstly affects the SCS summer monsoon, which is far

away from the plateau, rather than the onset of Indian monsoon, which is near, making the summer monsoon break out firstly in the SCS but not in India. Li and Yanai (1994) believed that the thermal advection from the Tibetan Plateau affected the warming of the East Asian Continent, thus produced the north-south thermal contrast between the land and the sea to impact the onset of SCS summer monsoon. In the SCSMEX, a lot of investigators pointed out that the upper level South Asian anticyclone was attracted by the heating of Tibetan Plateau and jumped northward from the SCS to Indo-China Peninsula, and then created north-south temperature gradient and resulted in the formation of the southern branch of summer easterly jet. He et al. (2000) showed by numerical simulation experiments that the land heating of Indian Peninsula promotes a cyclonic cell on its east side to enhance the Indo-Myanmar trough or BOB trough and is advantageous to the summer monsoon breaking out firstly in the SCS instead of in India.

Based on the ECMWF data from 1980 to 1986, Chang and Chen (1995) studied the development of the southwest wind surged at 850 hPa over the north part of SCS and found that the acceleration of the west wind in May depends on the mid-latitude baroclinic frontal system, which moves southward to the coastal areas of China and stagnates there. Then the southwest airflow keeps on the south side of the frontal system and maintains the moisture transport from Indo-China Peninsula. There are twice west wind surging in May and the first one corresponds to the onset of the summer monsoon. Based on this viewpoint, it can be deduced that the mid-latitude frontal system associated with the onset of the early summer rainy season is one of the triggering mechanisms of the onset of the SCS summer monsoon. Later, Liu et al. (2002) pointed out that the southward movement of the mid-latitude frontal system is related with the eastward propagation of the Rossby wave excited by convective activities over the BOB. Ding and Liu (2001) and Chen Longxun et al. (2000) also found the close relationship between the onset of the summer monsoon over the north part of the SCS and the cold air activities in mid-latitudes in 1998. They further pointed

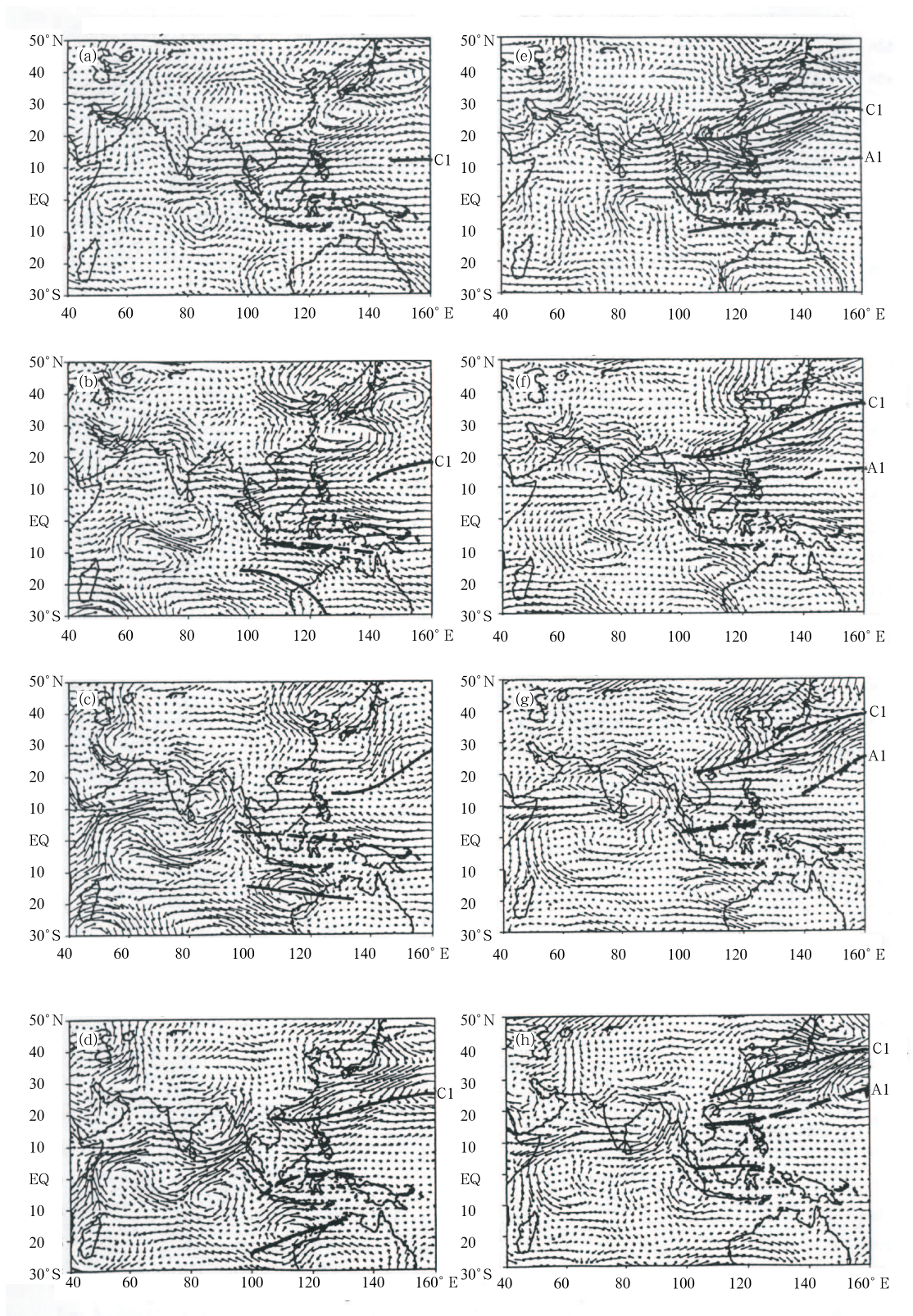


Fig.8. 850-hPa filtered 30-60-day wind fields for May 5 to June 9, 1998 (Chen et al., 2001). (a) - (h) are for May 5, 10, 15, 20, 25, 30, June 4, and 9, respectively. C1: cyclonic disturbance. A1: anticyclonic disturbance.

out that the cold air events enhanced the low-level west wind and convective activities rapidly.

4. The development of the mesoscale convective system over the SCS during the onset of summer monsoon

The onset of the SCS summer monsoon is characterized by the rapid development of convective activities and the quick increases of rainfalls over the SCS. During the SCSMEX, a series of organized mesoscale convective systems (MCSs) were observed using the dual Doppler radar array deployed in the northern SCS (Lau et al., 2000). Both the ISS comprehensive sounding system in Dongsha Island and the intensive sounding observation by Shiyan No.3 experimental and the Kexue No.1 scientific observation ships also captured the evolution of the stratification and wind fields before and after the convective activity break out. The zonal wind and θ_{se} (Ding et al., 2004), which were ob-

served by the Shiyan No.3 experimental and the Kexue No.1 scientific observation ships during the onset of the SCS summer monsoon in May 1998, showed the apparent potential instability in stratification before the onset of the northern SCS (Figs.9a, c). There was a deep dry layer in the middle of the troposphere and $\partial\theta_{se} > 0$ below 600-700 hPa, showing the potential instability. The west wind established rapidly through the whole troposphere as the summer monsoon onset (15-21 of May). At the same time, the potential unstable level disappeared, implying that the convective activities broke out as the release of quantities of disable energy. Then, the wet and neutral stratification maintained. The onset of the convection in the southern SCS was not as intensive as that in the northern SCS, but the continuous decrease of the potential instability could also be observed as the weakness and transformation to west wind of the mid-low east wind.

According to rainfalls retrieved from the dual

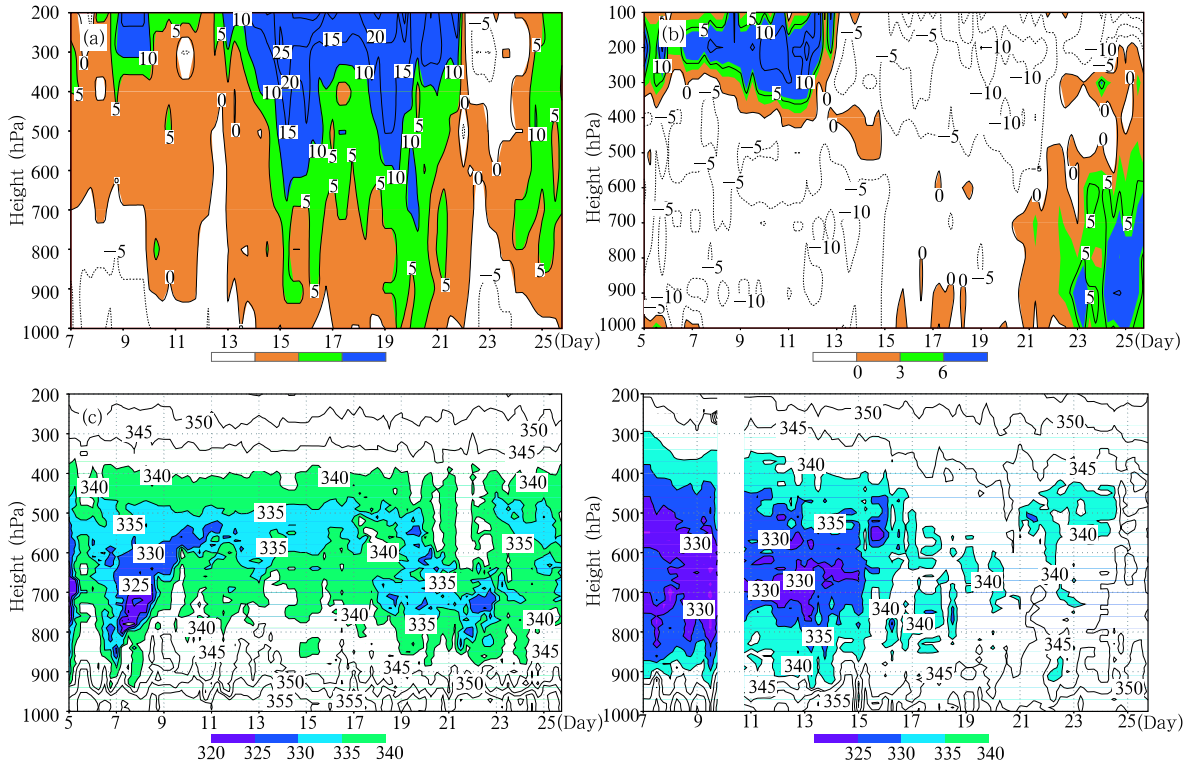


Fig.9. Height-time cross-sections of zonal wind and pseudo-equivalent potential temperature at R/V Shiyan # 3 (a, c) and R/V Kexue # 1(b, d) in 1998. For (a) and (b), the full lines denote westerly wind and the dashed lines denote the easterly wind. The westerly wind is shaded. The units are $m s^{-1}$ and the contour interval is 5 units. For (c) and (d), the values below 340 K are shaded and the contour interval is 5 units. R/V Kexue # 1 and R/V Shiyan # 3 indicate the research vessel which were stationary at $6^{\circ}15'N$, $110^{\circ}E$ and $20^{\circ}29'39''N$, $116^{\circ}57'58''E$ during the IOPs of 1998, respectively.

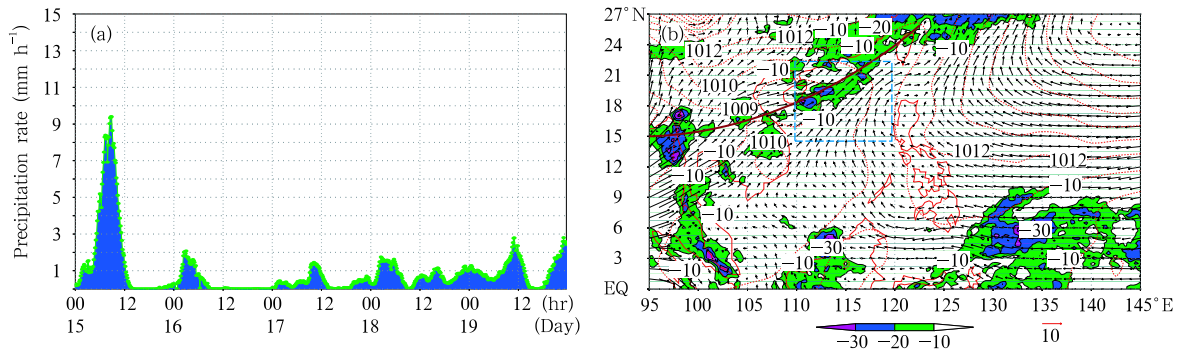


Fig.10. (a) Retrieved precipitation per ten minutes from dual-Doppler Radar during May 15-19 in 1998, which was mainly resulted from mesoscale convective systems (MCSs) (unit: mm h^{-1}). (b) 850-hPa wind field (unit: m s^{-1}), sea-level pressure (unit: hPa), and TBB (unit: $^{\circ}\text{C}$) during May 15-19 in 1998. Dashed box: the region investigated in the northern SCS; bold black line: monsoon trough.

Doppler radars observations during the SCSMEX, about 8 evident mesoscale rainbelts, which were mainly resulted from MCSs (Fig.10a) (Lau et al., 2000), were observed during 15-19 May. Their mean life spans were 6-12 hours and some single ones' were even longer. These MCSs could be divided into three types according to their migration characters: the type of migration from northwest to southeast; the type of migration from southwest to northeast, and the stationary type. Formations of these MCSs were closely related to the large-scale circulations during the summer monsoon onset. Especially, the establishment of the monsoon trough and the shear line at low levels supplied advantageous synoptic and dynamic conditions for the formation and maintenance of the MCSs (Fig.10b). Moreover, the persistent and extensive mesoscale convective activities produced obvious feedbacks to the large-scale circulations through the cumulus heating. The release of the latent heat driven by enhanced convective activities resulted in intensive atmospheric heating over the northern SCS ($Q_1 > 0$, $Q_2 > 0$) by calculations (Johnson and Ciesielski, 2002). Correspondingly, the surface pressure decreased while the monsoon trough as well as the southwest monsoon current on its south side strengthened. This positive feedback mechanism between the monsoon trough and MCSs was favorable for the eastward retreat of the subtropical high in mid-upper layer of the troposphere over the SCS and the reversal of the meridional temperature gradient over the SCS and Indo-China Penin-

sula.

5. The teleconnection and intraseasonal oscillation (ISO) of the SCS summer monsoon

5.1 ISO of the SCS summer monsoon

The activity and variation of the SCS monsoon are characterized by multi-time scale variability, especially low-frequency oscillation. It is clearly shown that there dominantly exists quasi 20-70-day (intraseasonal) low frequency oscillation of the SCS summer monsoon activities through the SCSMEX (Ding and Li, 1999; Zhu and Xu, 2000). One of the cases in Fig.11 indicates that 20-40-day and 50-70-day are two dominant oscillation periods in 1992 whereas 30-50-day in 1998, based on analysis of zonal wind or OLR. Thus the characteristic of low frequency oscillation of the summer monsoon activity is very evident.

In addition to the low frequency oscillation of the SCS summer monsoon, the atmosphere ISO exerts distinct influence on the activities of the SCS monsoon, with the close relationship between the onset of SCS summer monsoon and the ISO, depicted in Section 2. Li and Wu (2000), Mu and Li (2000) pointed out the existence of 30-60-day low frequency oscillation in the SCS, by analyzing the temporal evolvement of 850-hPa zonal wind and the evolution of low frequency kinetic energy, and the SCS summer monsoon onset is closely related to the ISO in this region, with the low frequency west wind emerging two days earlier than

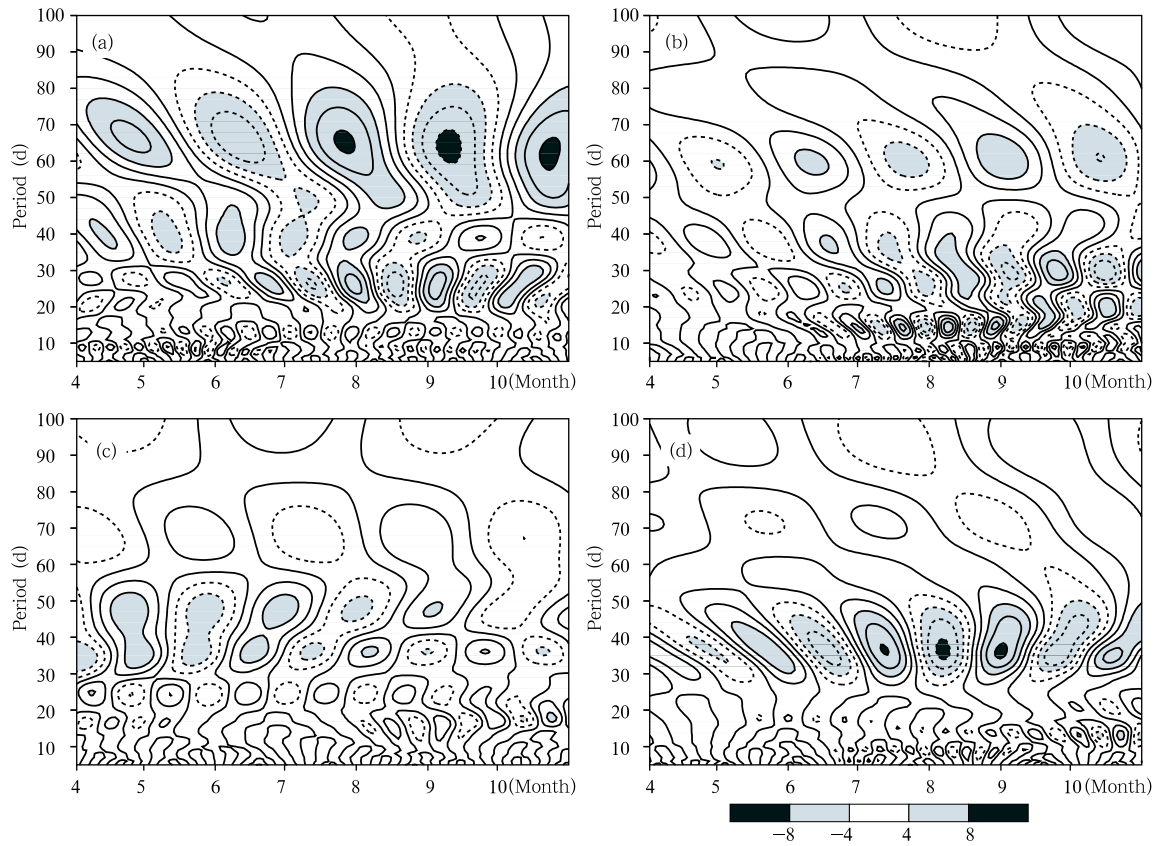


Fig.11. Wavelet analysis of 850-hPa mean zonal wind (a, c) and OLR (b, d) in the SCS (5° - 20° N, 105° - 120° E) for 1992 (a, b) and 1998 (c, d) (Zhu and Xu, 2000).

monsoon onset. Furthermore, it is seen, from the change of the low frequency zonal wind, that the intensification of the low frequency west wind over the SCS is attributed to the westward propagation of the low frequency from the east and the intensification in situ (figure omitted). While the eastward propagation of the low frequency wind from the Indian Ocean may affect the monsoon development after its onset.

It is also demonstrated by the daily horizontal distribution of 850-hPa 30-60-day low frequency kinetic energy before and after the SCS summer monsoon onset (during 18-23 May) in 1998 (figure omitted). The characters of extra intensification in low frequency kinetic energy center over the ocean surface to the east of Philippines with the monsoon coming, continual westward expansion of the activity domain and fierce strength over the SCS, despite little movement of the center, reflect the important impact of intensive growth and westward expansion of 30-60-day low fre-

quency oscillation activities to the east of Philippines on the intraseasonal atmospheric oscillation and summer monsoon onset over the SCS. It is true in 1980 and 1986. For reasons above stated, we can infer the dominant role of the intense development and westward extension of 30-60-day low frequency kinetic energy to the east of Philippines in the intraseasonal atmospheric oscillation and the onset of summer monsoon.

The corresponding investigation indicates that the atmospheric ISO has an important influence on the variations of East Asian summer monsoon (Li et al., 2001). The composite analysis for the strong and weak SCS summer monsoon years shows distinctly anomalous features of the atmospheric circulation situation at the lower (850 hPa) or upper (200 hPa) level of troposphere. The difference during June-August between strong and weak summer monsoon years is obvious, with stronger west wind between 5° N and 20° N, stronger east wind between 5° S and 20° S and stronger

cyclone circulation over the north-east of the SCS in the compositively anterior 850-hPa stream field, and with strong (weak) ISO stream field and strong (weak anti-) cyclone circulation corresponding to strong (weak) SCS, the SCS summer monsoon-West Pacific areas in the composited stream field of 850-hPa intraseasonal atmospheric oscillation. Therefore strong atmospheric ISO activities and low frequency cyclone circulation mainly contribute to the formation of strong cyclone circulation as one of the primary features of strong SCS summer monsoons.

Likewise, the composited stream fields of the strong and weak SCS summer monsoon also have some differences (figure omitted). Strong SCS summer monsoon is characterized by abnormally strong South Asian high which is located at the northwest of the normal position and much stronger anti-cyclone circulation which has a seasonal oscillation feature over the Tibetan Plateau.

5.2 *Teleconnection mode of the SCS summer monsoon*

Both data analysis and numerical simulation clearly indicate that the anomaly of the SCS summer monsoon has obvious influence on summer monsoon rainfall in East China. A strong (weak) SCS summer monsoon usually leads to less (more) precipitation over the middle and lower reaches in the Yangtze River Basin, and more (less) precipitation in North China, which demonstrates the abnormal SCS summer monsoon's influence on precipitation of flooding period in China. The influence of abnormal SCS summer monsoon on climate in China and other East Asian areas has visible wave train feature of teleconnection. By data analysis and numerical simulation, Li and Zhang (1999) pointed out that the abnormal SCS summer monsoon has influence on the weather and climate in not only China, Korean, and Japan, but also America through East Asian-Pacific-North America (EPA) teleconnection (wave train). Figure 12 is the correlative patterns for 500-hPa height fields over Northern Hemisphere for the strong and weak SCS summer monsoon, which the reference point is 15°N, 112.5°E. Different EPA wave trains can influence the weather and climate of both East Asia and North America.

Recently, American scientists studied the teleconnection (influence) between North America and East Asia regarding the summer rainfall in the middle part of United States, and they got the monsoon mode (teleconnection wave train) affecting drought and flooding in summer in United States which is in accordance with the EPA wave train put forward by us (Lau and Weng, 2002).

6. Flux exchange on the air-sea interface

The flux observation over the SCS is a weakness in tropic ocean areas. Only a short time heat flux observation was undertaken on Nansha Zhubijiao Platform before 1998. The SCSMEX in 1998 employed northern and southern flux observation arrays and measured in-phase surface fluxes using observation tower and fixed and moving ships. The air-sea flux observation tower on Xisha Yongxing Island accomplished three observation experiments in 1998, 2000, and 2002, respectively, and obtained the data of wind, temperature, moisture on the sea surface, upward and downward short and long wave radiation, wind velocity and moisture pulse, temperature of sea surface and part wave, which established good foundation for the research of air-sea interface process, flux parameterization and further understanding energy and water cycle (Yan et al., 2000; Jiang et al., 2002; Yan et al., 2003).

(1) The processes of air-sea flux exchange and the characteristics under the influence of different synoptic system

Accompanying a sudden changes of wind direction, wind velocity, cloud fraction, precipitation, moisture, and sea surface state, radiation flux changes obviously during the period of outbreak of the SCS, especially solar short wave radiation and sea surface net radiation. Solar radiation arrived at sea surface accounts for about 2/3 and even only 1/2 during the period of convective heavy rainfall and continuous rainfall respectively prior to monsoon onset. The changes of long wave radiation of atmosphere and sea surface long wave radiation are relatively steady; the change of the latter is even less. Cloud fraction is small before south-west monsoon onset. The daily mean of net radiation on sea surface is over 200 W m^{-2} . Cloud

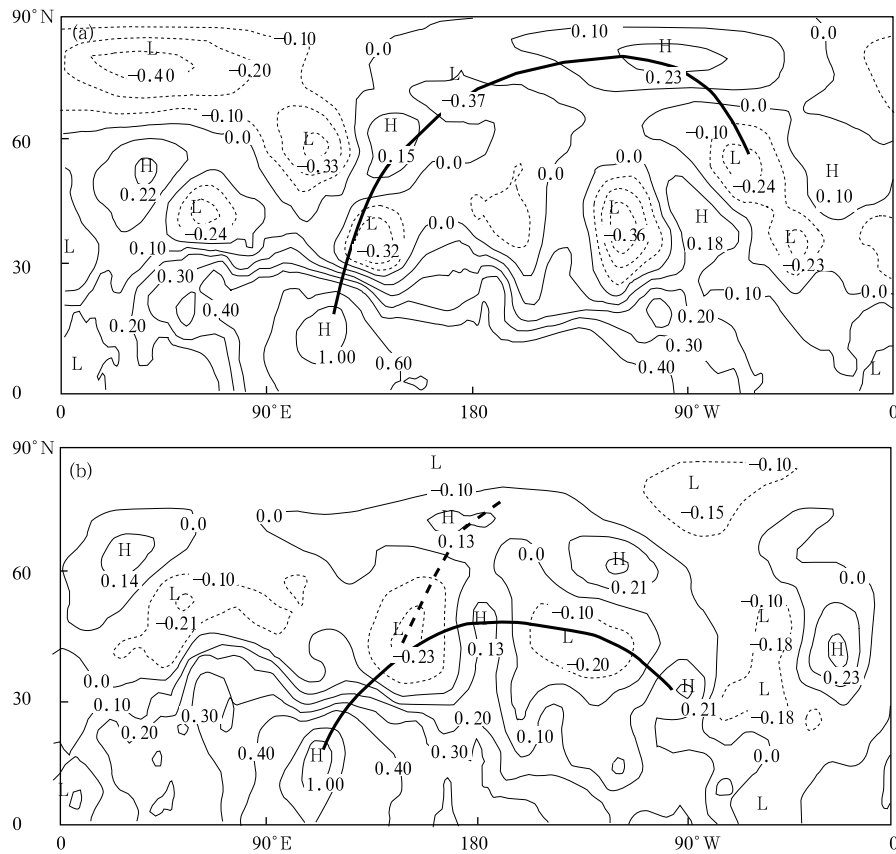


Fig.12. Correlative patterns for 500-hPa height fields in Northern Hemisphere for strong SCS summer monsoon (a) and weak SCS summer monsoon (b) (see Li and Zhang, 1999). Base point is 15°N, 112.5°E.

fraction increases in monsoon onset period with daily mean of only 150 W m^{-2} and reduces to 95 W m^{-2} during the period of rainfall, which is only 42% of that before monsoon onset.

Sensible heat flux transportation is mainly from atmosphere to ocean and the mean sensible heat flux is 7.8, 5.2, and 5.2 W m^{-2} in the observation time of 1998, 2000, and 2002, respectively. The variation trend of daily sensible heat flux is obvious before the onset of SCS monsoon. Average sensible heat flux slightly increased after the onset of monsoon (including the phases of the onset, the low pressure development, and southwester), but its value obviously increased during rainfall process, ever reaching $40\text{-}50 \text{ W m}^{-2}$ in the course of heavy precipitation. However, sensible heat flux is relatively low during the period of southwester, which is caused by the decreasing of air-sea temperature difference due to sea water sufficiently mixing with large wind velocity inducing wave

appearing on sea surface.

Average latent heat flux is 110, 85, and 95 W m^{-2} during the observation period in 1998, 2000, and 2002, respectively. The variation of latent heat flux is relatively small with the high daily variation in daytime and low daily variation in deep night before monsoon onsets and the change of latent heat flux increases after monsoon onsets. Latent heat flux obviously reduces in the process of rainfall and the larger value appears during the phases of southwester and the broken period of SCS monsoon.

The average net ocean heat gain is 71.8 and 76.6 W m^{-2} during the observation period in 2000 and 2002, respectively, but the difference of the average is quite great in different synoptic phases. The average reaches 126 W m^{-2} prior to the onset of SCS monsoon, which is distinctly higher than the average. The cloudiness increases after monsoon onsets and net radiation flux reduced to 2/3 of the average, net ocean

heat gain may be near to zero or negative value some time when the sensible heat and latent heat flux are excluded from ocean and the lost heat fluxes from sea surface in the process of rainfall are considered. Table 1 is mean sea surface fluxes during different weather conditions in 2002.

Air-sea flux is measured with research ships Shiyan #3 and research ships Kexue #1 (Qu et al., 2000). All kinds of air-sea flux parameters were calculated using the eddy method. Further information can refer to the paper written by Ding et al. (2004), in which the detailed observational results have been described.

(2) Comparison of heat exchange among the SCS, the BOB, and the West Pacific Ocean Warm Pool before and after the onset of monsoon

The SCS is adjacent with the ocean areas such as the BOB and the West Pacific Ocean Warm Pool. Although they locate at tropical belt, heat quantity and moisture exchanges have different features. Table 2 is the experimental results of ships observations in West Pacific Warm Pool, experiment satellite Nauru-99 observations, air-sea interaction observations in the BOB. Pacific TOGA-COARE includes two phases: calm period before westerly bursting in November 1992 and the onset period of westerly from December 1992 to January 1993. Air-sea interaction experiment in the BOB involves three phases: the weak wind period before the onset of southwesterly monsoon in 10-15 May 1999; the onset period of southwesterly monsoon in 21-26 May; and the broken period of southwesterly monsoon in 12-23 September.

Table 1. Mean sea surface fluxes during different weather conditions for 2002 (W m^{-2}) (see Yan et al., 2003)

Weather stage		V (m s^{-1})	R (mm)	N 1/10	Q_s	Q_b	H_s	E_L	Q_n
Before onset (1)	20-30 Apr.	4.2	0.0	4.3	277.2	-58.0	-5.8	-86.3	127.1
Before onset (2)	9-13 May	4.1	0.0	3.2	290.5	-60.7	-4.2	-101.8	123.8
Monsoon onset (1)	14-18 May	6.1	79.0	7.3	194.0	-41.4	-5.0	-97.2	50.4
SW strong wind (1)	19-23 May	7.6	0.0	7.1	222.8	-40.2	-2.7	-100.6	79.3
Monsoon Low (1)	24-29 May	3.3	126.0	8.9	181.2	-39.7	-11.1	-89.2	41.2
SW strong wind (2)	30 May-2 Jun.	7.5	0.0	7.4	232.6	-42.3	-4.9	-96.8	88.6
Monsoon Low (2)	3-6 Jun.	5.9	47.4	8.6	126.9	-31.9	-5.2	-71.2	18.6
SW strong wind (3)	9-12 Jun.	8.5	0.0	6.7	264.9	-45.4	-3.5	-124.3	91.7
Monsoon break	13-18 Jun.	6.5	15.7	5.8	253.1	-51.7	-6.4	-125.3	69.7

(V : wind velocity, R : precipitation, N : total cloudiness, H_s : sensible heat flux, E_L : latent heat flux, Q_s : net short wave radiation absorbed by ocean (total solar radiation Q_s : short wave radiation reflected by ocean surface Q_{sw}), Q_b : net long wave radiation (atmosphere long wave radiation Q_{LS} , ocean surface long wave radiation Q_{LW}), and net heat revenue and expenditure for ocean Q_n . Net heat revenue and expenditure for ocean was calculated by the following formula: $Q_n = Q_s - Q_b - H_s - E_L$, flux absorbed (liberated) by ocean is positive (negative) value.

Compared Table 1 with Table 2, it is indicated that there are some discrepancies among the different ocean surfaces. Latent heat flux increased more obviously in the onset period of westerly at the West Pacific Warm Pool and monsoon at the BOB than that before the onset of those, but decreased in the SCS to some extent. The variation of latent heat flux is so obvious that there exists relatively large negative ocean heat net income and outlay during the onset period of monsoon in the BOB; less negative value in

westerly onset period in the West Pacific Warm Pool; positive value in the onset period of the SCS monsoon. Net long wave radiation increased in the monsoon onset period in the West Pacific Ocean, but reduced in the BOB and SCS. The results show that latent heat flux in the onset period of southwesterly monsoon increases more intensively than that before the onset of monsoon in the BOB comparing with the West Pacific Ocean Warm Pool and the SCS.

(3) The variations of sensible and latent heat flux

and momentum flux along with the wind velocity, the air-sea temperature difference (ASTD), and the air temperature (water temperature)

The relationships are not identical between the variation of sensible, latent heat flux, the momentum flux, and the meteorological factors. The sensible heat flux (SHF) almost does not change along with the increase of wind velocity when it is less than 10 W m^{-2} . However, the SHF augments obviously along with the increase of wind velocity when it is greater than 10 W m^{-2} . There is an obvious positive correlation between the SHF and the ASTD. The correlation coefficient is greater than 0.9. The relationship is closer, especially when the ASTD is below 2°C . The SHF increases correspondingly along with the augment of the ASTD. Furthermore, there is an obvious negative correlation between the SHF and the

air temperature. Because the air temperature over the ocean is lower than the sea-surface temperature, the SHF decreases correspondingly along with the increase of the air temperature and the decrease of the ASTD. However, the latent heat flux (LHF) is positive correlated with the wind velocity, the ASTD, and the sea-surface water temperature, and there is a closest relationship between the LHF and the wind velocity. The correlation coefficient reaches 0.6. The LHF increases rapidly along with the enhancement of velocity. And their relationship can be fitted by linear relation: $E_L=8.18V+51.62$. The correlation between the LHF and the sea-surface water temperature is better. Therefore the LHF increases correspondingly along with the enhancement of sea-surface water temperature.

The average value of the sea-surface momentum

Table 2. Experiment results of air-sea interaction in the West Pacific Warm Pool and Bay of Bengal (W m^{-2}) (see Yan et al., 2003)

Experiment		Q_s	Q_b	H_s	E_L	R	Q_n
Pacific	TC-stage 1	222	-58	-7	-89	-1	65
	TC-stage 2	166	-66	-11	-117	-4	-12
Nauru	TC-stage 1	252	-63	-3	-87	-1	98
	TC-stage 2	211	-71	-8	-133	-3	-4
Indian Ocean JASMINE	stage 1	260	-49	-5	-115	-0	92
	stage 2	162	-31	-17	-162	-7	-89
	stage 3	229	-38	-3	-92	-1	96

flux in 2002 was 0.045 N m^{-2} , which was the same as the measure result of 0.0446 N m^{-2} during JASMINE-99 in the BOB. The relationship between the sea-surface momentum flux and the wind velocity is obvious. That is to say, the sea-surface momentum flux rises when the wind velocity enhances. The relation between the momentum flux τ and the wind velocity V is defined as:

$$\tau = 0.00185V^2 - 0.00559V + 0.01248. \quad (1)$$

(4) The calculation of the air-sea flux exchange coefficients

The exchange coefficients (EC), including the momentum EC (C_D), the sensible heat EC (C_H), and the latent heat EC (C_E), are important parameters to calculate the fluxes by means of the conventional observation and the whole transportation formula. These

coefficients can change rather largely along with the variation of the weather and the surroundings in ocean instead of a constant. All sorts of exchange coefficients under the neutral condition and a variety of weather conditions are proposed according to the calculation of the observation experiment data. The relationship between them and meteorological elements was also discussed. The mean C_{Dn} was $(1.029 \pm 0.16) \times 10^{-3}$ under the neutral condition during the experiment in 2002 with the value on the small (large) side before (after) the monsoon onset. The distribution of C_{Dn} along with the wind velocity can be fitted by a polynomial:

$$C_{Dn} = 0.00108 - 7.0996 \times 10^{-5}V_{10} + 1.3009 \times 10^{-5}V_{10}^2 - 4.4079 \times 10^{-7}V_{10}^3. \quad (2)$$

The whole momentum EC (C_D), which decreases rapidly (increases slowly) with the increase of wind

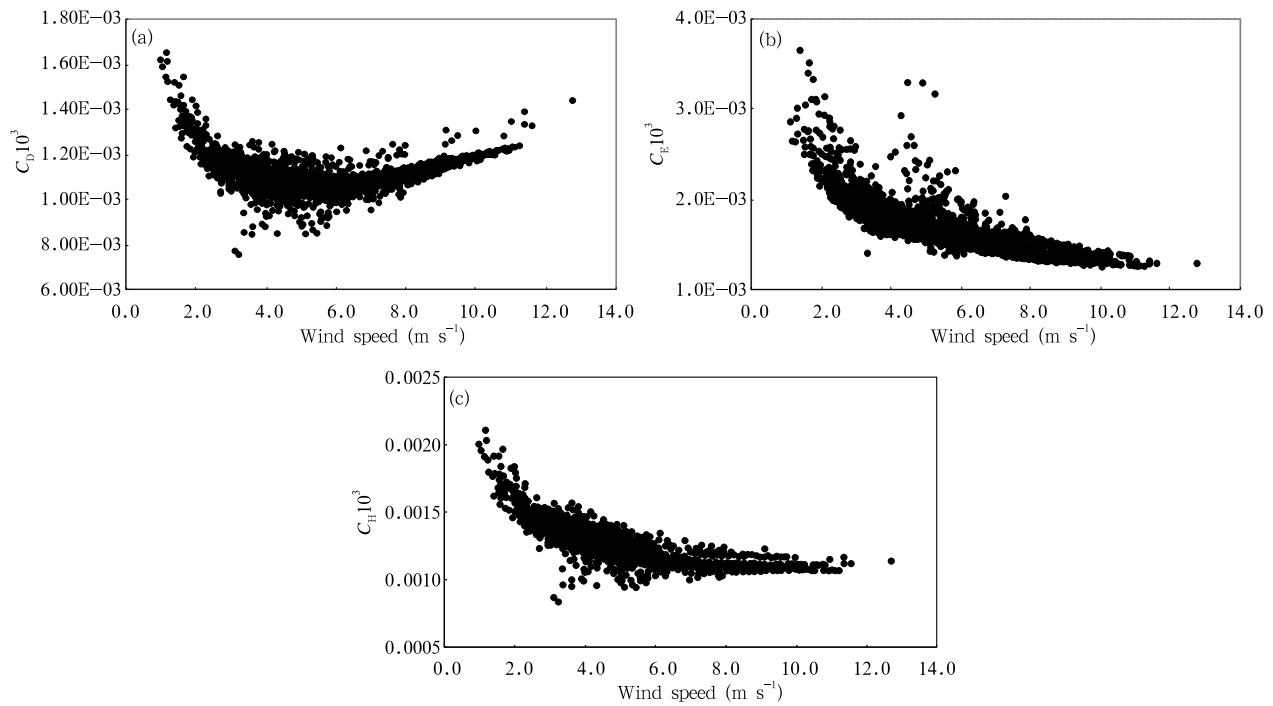


Fig.13. Change in momentum (a), latent heat (b), and sensible heat (c) exchange coefficient with wind speed obtained in the sea near Xisha Island during the SCSMEX (Yan et al., 2003).

velocity when the wind velocity is less (greater) than 5 m s^{-1} , namely smooth (coarse) flow, has a close relation with the wind velocity (Fig.13). On the other hand, C_H is positive correlated with the ASTD, especially when the ASTD is below 2°C , and obvious negative with the air temperature. Furthermore, C_E is closely linked to the wind velocity. C_E reduces rapidly (slowly) with the enhancement of the wind velocity when the wind velocity is less (greater) than 5 m s^{-1} , while C_E tends to a stable value when the velocity is greater than 12 m s^{-1} . Also, the ASTD influences the change of C_E . C_E increases correspondingly along with the enhancement of the ASTD when the ASTD is less than 2°C . But the correlation weakens when the ASTD is greater than 2°C . In the same way, the heat flux and the momentum EC have a polynomial (linear) relation with the wind velocity (ASTD).

7. Some dynamics and thermodynamic features of the upper layer ocean under the action of the SCS monsoon

SCS monsoon experiments highlight to focus on

a lot of researches, including the interaction between the SCS circulation and the SCS monsoon, the spatial-temporal evolution of mesoscale vortex, the stratified structures of the upper layer of the SCS and their low frequency variability, the remote sensing analysis associated with the mesoscale dynamics and the interaction between the atmosphere and the ocean, and so on. The theoretical system of the dynamics process of tropical mesoscale ocean in the SCS is preliminarily set up.

(1) According to the diagnosis and analysis of the SCS observation data, the intense warm event in the SCS and the corresponding ENSO pattern anomaly of circulation were found (Fig.14), which happened from the spring and summer of 1997 to the spring of 1999 in the SCS and was at the first place with the strongest intensity and the longest duration period in recent several decades. The occurrence and development of the warm event in the SCS corresponded with that of the ENSO event in the eastern tropical Pacific. And almost at the same time both of them arrived at the maximum in the winter of 1997/1998 (exactly about

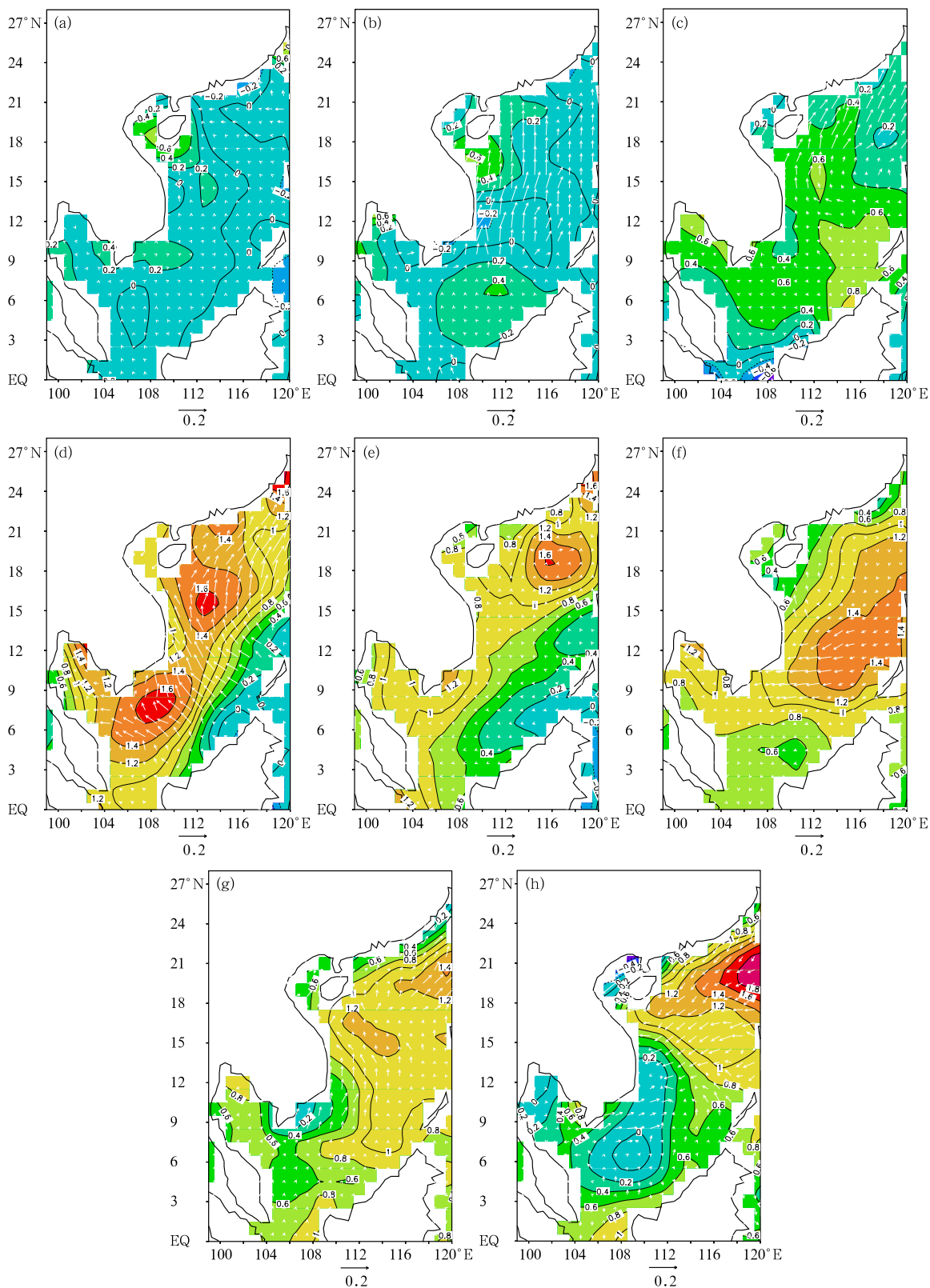


Fig.14. Seasonal mean SSTA and sea surface stress for 1997/1998 warm event. (a) March-May, (b) June-August, (c) September-November 1997; (d) December 1997-February 1998; (e) March-May, (f) June-August, (g) September-November 1998; and (h) December 1998-February 1999.

in January 1998). The sea surface temperature anomaly (SSTA) of a great part of the SCS maritime domain exceeded more than 1°C . The summer (winter) monsoon of 1997 was stronger (weaker) in East Asia, thus the sea surface wind anomaly in the SCS occurred the coherent southerly anomaly. The warm air advection, which is generated by the southerly anomaly, played an important role in the development process of the SCS SSTA. At this stage, there was no systematic sea surface height anomaly (SSHA) in the middle of the ocean basin and the adjustment of the thermocline was not obvious. Subsequently the southerly anomaly over the SCS reduced and even occurred the northerly anomaly in the summer of 1998 for the weaker SCS summer monsoon in 1998. At this time the high SSTA was located in the northern deep-water region and around the gulf of Thailand. Furthermore, the thermocline deepened and protruded downward obviously. The convection mode induced by SSHA, which is in the middle of ocean basin and maintains the basin-scale circulation system, made SSTA in the SCS enter a maintenance stage. The SSTA in the southern SCS started to subside until the winter and spring of 1998/1999. The warm event finished in May 1999.

(2) In respect to the inter-annual variation of the circulation in the SCS, the analysis of the stream function anomaly field during the period of EL Niño and La Nina has been done. The anomaly in the summer mainly manifested the circulation itself enhancement during the period of El Niño, that is to say, the cyclonic vortex in the south and the anti-cyclonic one were both strengthened, nevertheless the cyclonic vortex was weakened in the whole SCS in the winter. On the other hand, in the process of La Nina, the influence on the circulation mode in the summer mainly focused on the northern SCS, viz., the weakening the cyclonic vortex in the north. However the cyclonic vortex in the whole of the SCS was reinforced in the winter. On the basis of the above cyclonic and anti-cyclonic vortex intensity change, the inter-annual variation of the SCS circulation provided the qualitative dynamic explanations for the inter-annual variability of SCS SST and enthalpy.

(3) (a) With the seasonal structure on the upper ocean circulation in the south of SCS, it was observed that the sub-basin scale vortex with the reverse direction between the summer and the winter, eastward off-shore current in the summer and the vortex dipole structure in the west of SCS existed. (b) The observations and the numerical simulations verified that the wind-driven circulation mainly happened in the south of the SCS and an anti-cyclonic vortex produced and developed at the Nansha trough, then propagated westward and decayed in the end, which was of about 50-day period. (c) In particular, the high resolution model revealed that the boundary-trapped Kelvin wave and westward propagating Rossby wave from the eastern boundary played an important role in establishment of the SCS basin-scale circulation state (Fig. 14). All the above facts brought forward the establishment mechanism of the ocean circulation of the SCS monsoon nature. Then we estimated the adjusted characteristic time scale of the ocean large-scale circulation in the SCS upper layer and the westward propagating Rossby wave from the eastern boundary. And (d) the viewpoint about the horizontal large-scale fluctuation of the oceanic circulation establishment and adjustment of the SCS monsoon nature was different from the former response mechanism of the local ocean to the wind stress and its vorticity forcing (Fig.15).

(4) It is known that the SCS is a notable ocean stratified region. The ocean-stratified structure was examined (Fig.16). The ocean meridional overturning circulation in the SCS exposed to conditions of the ideal submarine topography was reproduced, and results showed the meridional overturning circulation flux was about 0.7 Sv. The standpoint was brought forward that there was a distinct potential vorticity pool in the seasonal thermocline, and that the water of the mixed layer went into the upper layer of the seasonal thermocline and moved along the vorticity isopotential in the equidensite water layer. By the analysis of the climatological thermohaline data, some conclusions were given as follows: (a) the spatial-temporal distribution characters of the SCS mixed and barrier layer were shown; (b) the seasonal variation of the mixed layer's depth and the barrier layer's intensity

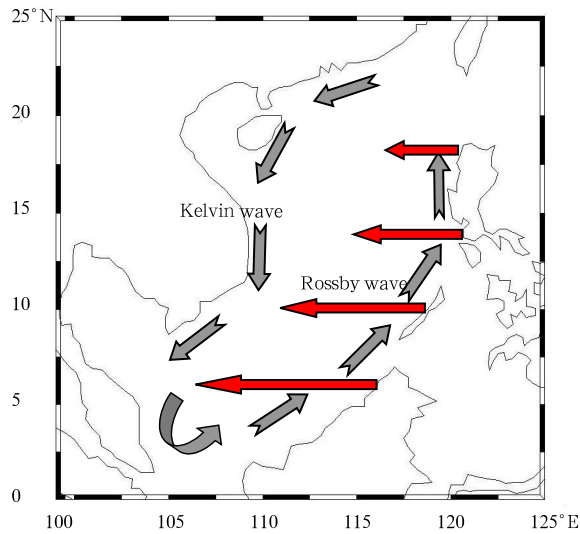


Fig.15. The important role of boundary-trapped Kelvin wave (grey) and westward propagating Rossby wave (black) originating in the eastern boundary in establishment of the SCS basin-scale circulation state.

were constructed; (c) the internal-relations between the SCS thermocline and the thermal condition of the upper layer ocean were given; and (d) the three-dimensional configuration of ‘the SCS warm pool’ was given, which indicated the isothermal envelope surfaces of 28°C from April to November appeared in a pot-like pattern, with different sizes and depths, and the evolution processes of the warm water were indicated figuratively with the numerical experiment at the same time. Although the above research gave some elementary discussion on the dynamical characters of the SCS thermocline, from the other hand, it includes some crucial information about the circulation seasonal adjustment existing in the SCS thermocline from their morphologic dynamics, which showed that their evolution played an important intrinsic role in constraining the circulation variation in the SCS.

8. Numerical simulations of the SCS and East Asian summer monsoon

Scholars in China have gained lots of achievements in studying the numerical simulations of East Asian monsoon which include both global and regional

models (Zhao et al., 1995). However, global models cannot simulate and predict the regional climate very well. Selecting eleven global circulation models and making a unified appraisal of their simulating characteristics in East Asia (15°-60°N, 70°-140°E), Zhao et al. (1995) found that there are significant inconsistency when simulating the summer and whole-year precipitation and temperature, particularly precipitation in East Asia. The above results show that global models cannot well simulate the climate characteristics which correspond to the observation even for such a large region as East Asia. Although the large-scale background field plays a leading role to some extent, the special topography and the underlying surface often result in the special changes of regional climate due to the various causes of regional climate. As the horizontal resolution of the global models is low, it is difficult to depict in detail the forces and impacts of the meso- and small-scale topography, surface characteristics and other factors on the regional climate change, thus they often fail to well predict the regional climate change. Therefore, it is extremely necessary to do numerical simulations on the seasonal variations and anomalies of the East Asian monsoon using regional climate models. During the SCSMEX, RegCM2-NCC (Liu and Ding, 2003), RegCM2 (the 2nd generation of NCAR regional climate models) (Giorgi et al., 1993a, b), and the p - σ regional climate model of Nanjing University (Qian et al., 1988) are used to simulate both the seasonal variation of the SCS monsoon and the roles of several factors causing its anomaly.

(1) Numerical simulations on the seasonal variation of the SCS monsoon with p - σ regional climate model

The seasonal variation of the regional climate in China is associated with the switch of the prevailing airflows, and the monsoon characteristics are most evident in the lower-troposphere. Figure 17 presents time-latitude cross section of 850-hPa zonal wind averaged at 105°-120°E (the longitudes of SCS) from early February to late January in the following year, it can be seen that the northeast by east wind prevails in the

SCS in winter, while the southwesterly monsoon flow forms in May, then experiences the enhancing-weakening-vanishing processes. October is the transitional period of the SCS summer monsoon, and easterly controls this region afterwards. In terms of the Southeast China (21° - 30° N), the southwesterly exists all the year round, but it strengthens obviously after the onset of the SCS monsoon in May. The monsoonal southwesterly exists in the lower-troposphere in June and July, reaches the north of 30° N in August, and withdraws gradually from the higher to the lower latitudes. Therefore, the simulated seasonal variation of the prevailing airflows in East China is in general agreement with the reality.

(2) Simulations of the effect of the Tibetan Plateau snow on the monsoon climate

There are already many studies on the numerical simulations of the impacts of the Eurasian snow cover and the Tibetan Plateau snow on atmospheric circulation monsoon. But since these studies generally adopt global models, they often fail to depict in detail the responding characteristics of regional climate to snow anomaly. Based on a regional climate model RegCM2, Qian et al.(2003) simulated the impacts of snow anomaly on the climate of summer monsoon in China and made six sensitivity experiments. The control experiment uses the climatological mean meteorology fields and sea temperature fields in January as the initial fields, integrates from 1 January to 31 August, and utilizes the observation data of boundary forcing and sea temperature in corresponding time. Here we only give the difference fields of precipitation and 850-hPa wind in summer among the experiment of the increase of snow depth in the Tibetan Plateau in winter (DL), the experiment with the observational fields of June-August in 1998 as the boundary conditions (BN), and the control experiment (Fig.18).

It can be seen from Figs.18a, b that the increase of snow depth in the Tibetan Plateau in the winter favors (disfavors) summer rainfall in the Yangtze-Huaihe Valley (in the south of the lower reaches of Yangtze River, South China, and North China); the forces of the boundary flow fields of June-August in 1998 pro-

duce the same but more significant effect. Thus, these two factors contribute to the occurrence of floods in the Yangtze River in 1998. Such regional distribution of the precipitation anomaly is closely related to the weakening of monsoon. Figures 18c,d are the difference fields of 850-hPa wind among DL, BN, and the control experiment. It shows that when snow depth in the Tibetan Plateau in winter increases, the East Asian monsoon weakens, a convergence zone of wind anomaly forms to the northern Yangtze River, and divergence zones form on its both sides, which matches well with the positive and negative precipitation anomalies. The forces of the boundary flow fields of June-August in 1998 produce the same distribution, but its effects on the weakening of East Asian monsoon are more significant.

Snow anomaly in the Tibetan Plateau acts on the summer monsoon climate in China through the feedback mechanism (i.e., memory capability) between "moist soil" and atmosphere, which is just the major mechanism of the influence of snow anomaly in the Tibetan Plateau on precipitation in spring and summer in China. In other words, a long-term anomaly of soil moisture and the feedback between wet soil and the atmosphere are the essential physical mechanisms that the information of snow anomalies is 'memorized' by the land-atmosphere system and has a lasting effect on the subsequent climate. However, by the end of May, the increase of the surface water and decline of land surface temperature resulted from snow anomalies have already been very little (figures omitted), and single hydrological processes are no longer able to produce a significant impact on the later land-atmosphere system. Therefore, whether the changes of temperature and humidity in the land-atmosphere system caused by snow anomalies can be maintained to May of the monsoon onset, has become the key to strength of the influence of snow anomaly on the later atmospheric circulation. In 1998, the effect of plateau snow depth anomaly did continue until May, moreover, the circulation situation (boundary forcing) was appropriate, which both had remarkable impacts on the summer monsoon climate.

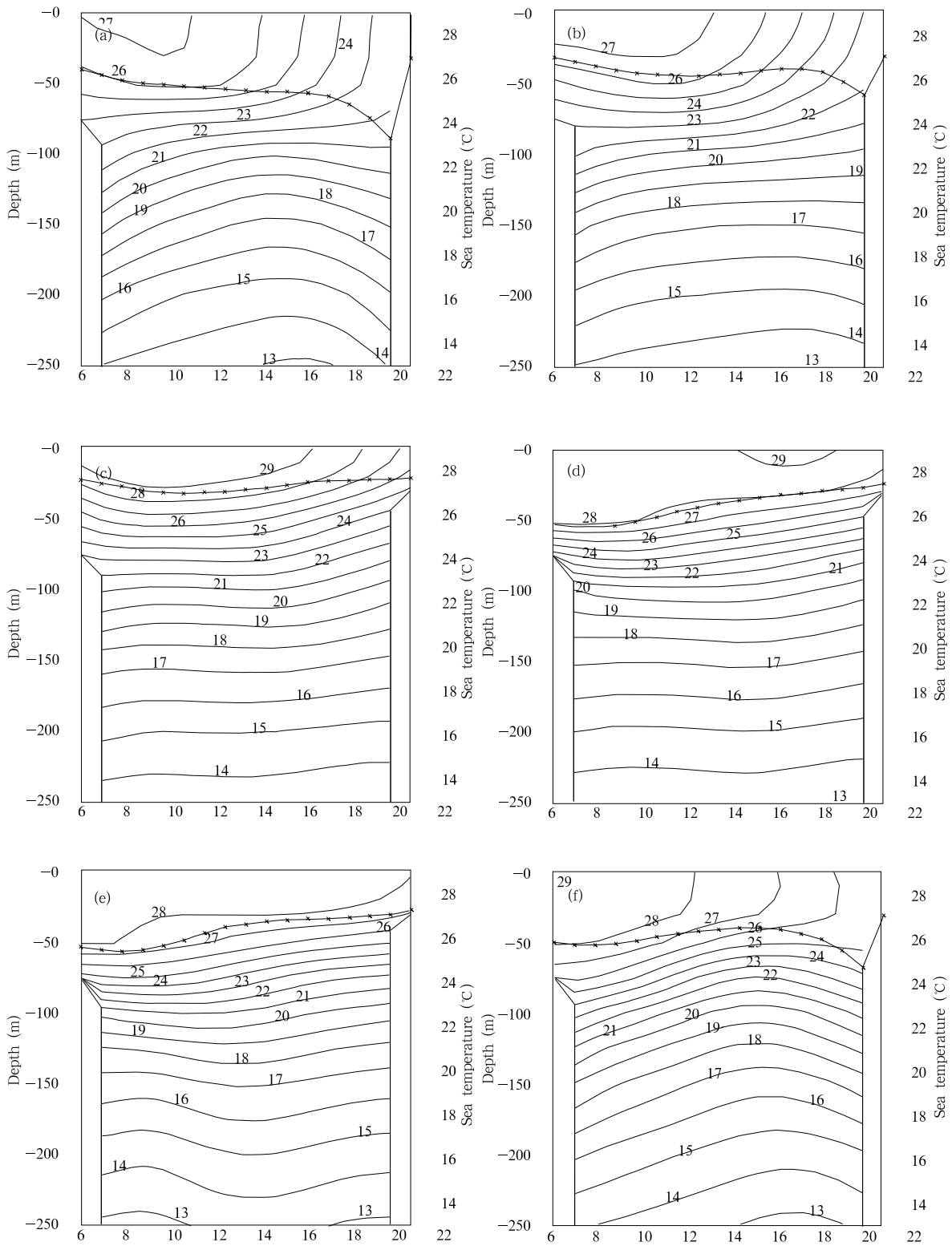


Fig.16. The ocean stratified characteristics of January (a), March (b), May (c), July (d), September (e), and November (f) along 115°E. Solid lines: isolines of sea temperature (unit: °C); and solid line with dots: depth of mixed layer (unit: m).

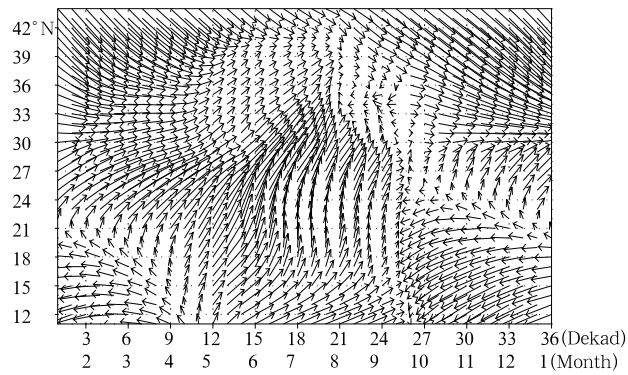


Fig.17. Latitude-time cross-section of 850-hPa zonal wind vector near 850-hPa model level averaged along (105° - 120° E) for the first ten days of February to last ten days of January in the following year (Qian et al., 2003).

(3) Simulation of the 1998 summer monsoon over the SCS based on coupled ocean-atmosphere regional climate models

By use of the improved RegCM2 and RegCM2-

NCC, Liu and Ding (2003) imitated the activity and precipitation process of the 1998 summer monsoon. Not only the whole process of the monsoon onset and active-break cycle, but also the process of the northward advance of the monsoon rain belt and the distribution of marked precipitation events during various precipitation periods were reproduced successfully.

A regional climate model named p - σ RCM is coupled to a regional ocean model, i.e., the South China Sea version (SCS-POM) of the Princeton ocean model (POM), to develop a new regional coupled air-sea model (p - σ +POM-CRCM) over East Asia and adjacent oceanic region, the processes for the climatologic onset and evolution of the summer monsoon are reproduced with it, and the summer monsoon in 1998 is also imitated to investigate the model performance and potential of the form and variation of East Asian climate monsoon (Ren and Qian, 2005).

It can be seen from latitude-time cross-section of

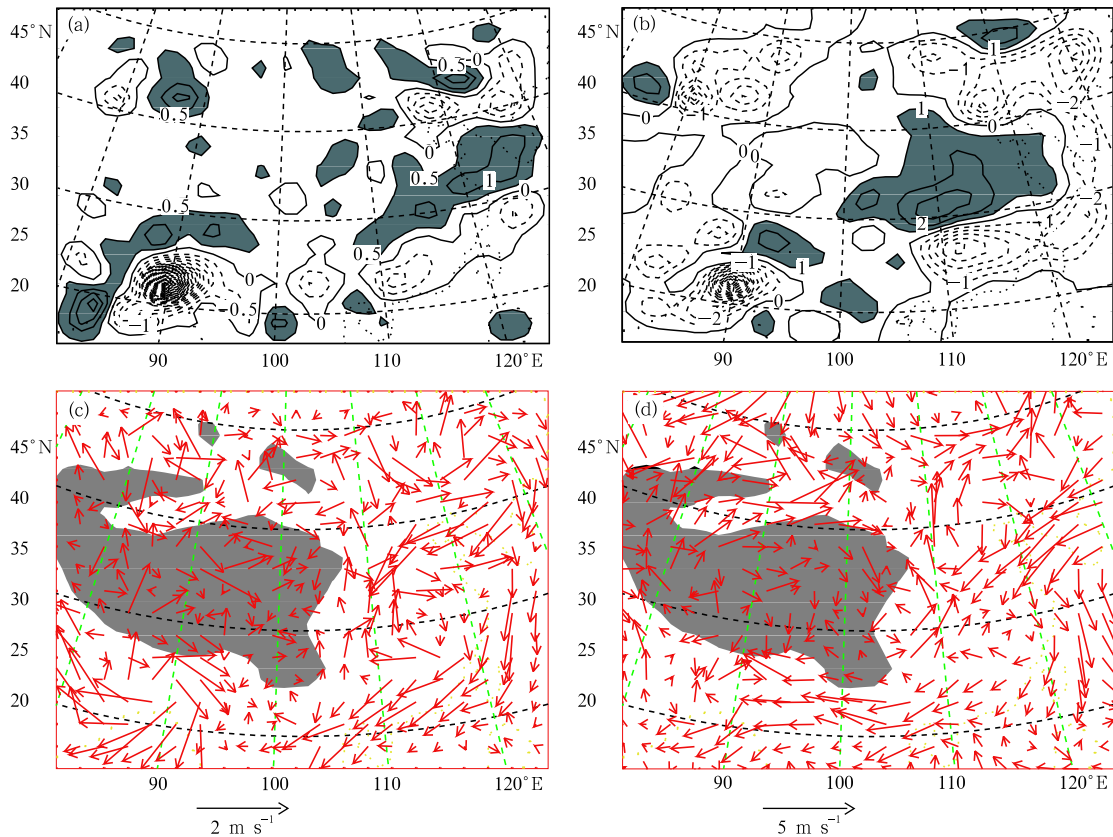


Fig.18. Change in summer precipitation (a, b, unit: mm d^{-1}) and 850-hPa wind fields difference (c, d, unit: m s^{-1}) caused by increase in snow depth in winter over the Tibetan Plateau simulated with RegCM2 (a, c) and boundary flow field forcing of May-August 1998 (see Qian et al., 2003).

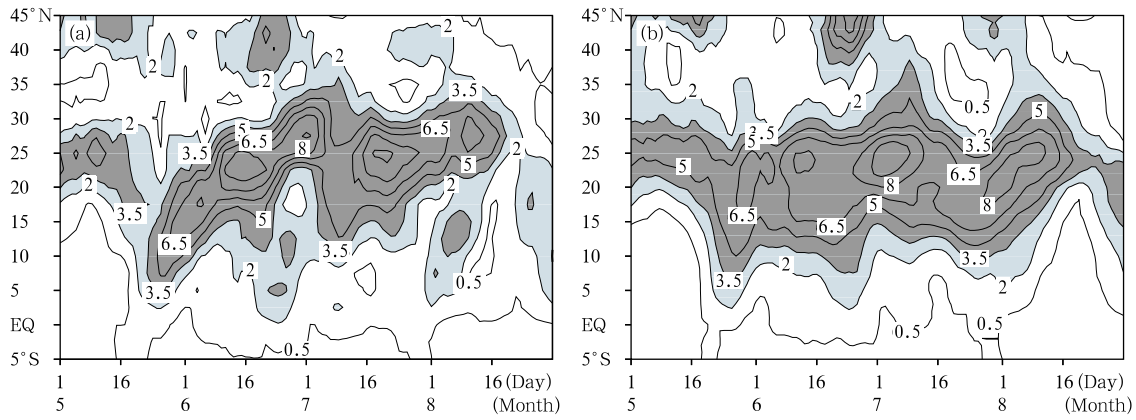


Fig.19. Latitude-time cross-section of low-level southwesterly wind along 105° - 120° E in 1998 (m s^{-1}). (a) Observed (850 hPa); (b) simulated (the 5th model level).

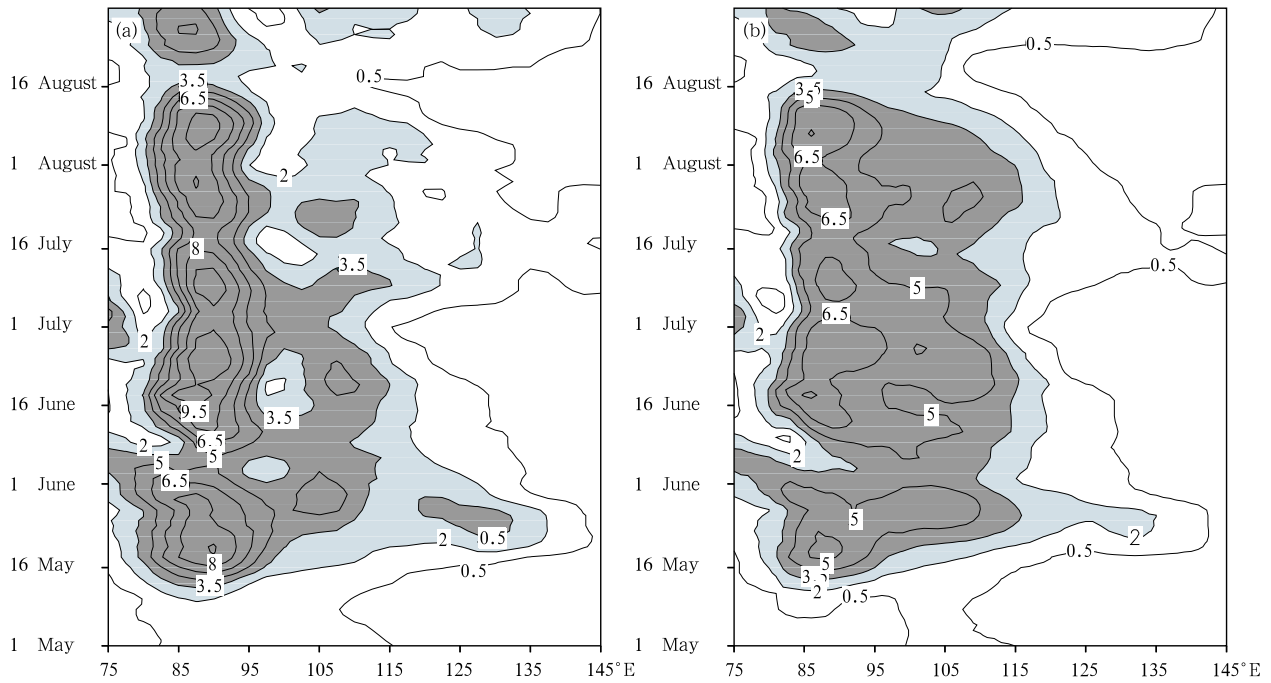


Fig.20. As in Fig.19, but for longitude-time cross-section of low-level southwesterly wind for 0° - 20° N zone in 1998 (see Ren and Qian, 2001).

low-level southwesterly wind along 105° - 120° E in 1998 (Fig.19) that the observed low-level southwesterly wind has three outbreak courses from south to north, respectively, in mid-late May, mid-late June, and the end of July-early August. The three northward outbreak courses are all simulated well, and the simulated intensity is also approximate to the observation fairly.

It is shown in some longitude-time cross-sections of low-level southwesterly wind along 0° - 20° N in 1998 (Fig.20) that the observed low-level southwesterly

wind has a process of enlarging eastward in mid-late May. In early June, the southwest wind is weakened, thereafter, maximum axis of the southwest wind remains at 95° E all along. These features have been simulated. However, the strongest southwest wind centre is slightly smaller than the observed, and after mid-July, the simulated maximum belt is broader than the observed.

During the simulation of the ocean elements in 1998 with p - σ +POM-CRCM, the simulation of ocean

currents is similar to the simulated results with POM driven separately by the observed data. Whereas, there is remarkable cold difference during reproducing the sea surface temperature. Analysis found that it is with the regional air-sea coupled model that climate drift is easier to occur during simulating surface sea conditions. The reason for this is possibly the disagreement in the surface heat fluxes produced by the atmosphere-ocean model with the observed. Surface ocean currents are sensitive to the error of wind stress and heat fluxes of the atmosphere model, which indicates that although the preliminary experiment of the coupled air-sea regional climate model is successful, there are many issues to be resolved.

9. Concluding remarks

The SCSMEX is a joint atmospheric and oceanic field experiment which aims at a better understanding of the onset, maintenance, and variability of the summer monsoon over the SCS. It is a successful large-scale international effort with many participating countries and regions cooperatively involved in the experiment. With the field observation in May-August 1998, a large amount of meteorological and oceanic data were acquired, which provides excellent datasets for the study of the SCS monsoon and the East Asian monsoon and their interaction with the ocean. They have been used in 4-D data assimilation by Japan, USA, Australia, etc., and compiled special datasets. Also, they were used in initial-value assimilations by China and Hongkong, which improved the forecasts of monsoon and precipitation at the various time-scales. On the other hand, all sorts of data acquired and collected in the SCSMEX were also utilized extensively in the study of the East Asian monsoon, and many notable achievements were gained. Here these results are summarized preliminarily. In short, the main research achievements are as follows:

(1) The Asian monsoon breaks out earliest over the Indo-China Peninsula and the SCS. It is the outcome of the seasonal variability of the large-scale atmospheric circulation forced by the specific heat sources, sinks, ISO, etc. From the viewpoint of the synoptic process, its onset bears an intimate relation

to the acceleration of the upstream lower-level west wind of the equatorial eastern Indian Ocean, development of a twin cyclone, reinforcement of low-pressure and strong development of convection over the BOB.

(2) During the SCS monsoon onset, a wide variety of organized mesoscale convective systems (MCSs) were observed over the northern SCS. They are closely related with large-scale circulations, and form a kind of positive feedback mechanism through condensational heating, which further enhances the onset of the tropical southwest monsoon.

(3) Two major low frequency modes, namely the 10-20-day and 30-60-day oscillations in the SCS were ascertained. On the background of seasonal variability, their phase locking of wet phases over the SCS plays a significant triggering role in the SCS summer monsoon onset, and the northward propagation of the low frequency oscillation can affect the occurrence of precipitation events over China and East Asian regions to a great extent.

(4) Convective activities over the SCS-West Pacific tropical area during the monsoon can stimulate stationary Rossby wave to generate the EPA teleconnection, the latter can not only influence East Asia, but also the downstream weather and climate in North America. Besides, the influences of the abnormal SCS monsoon on the precipitation over East China have been revealed. A strong (weak) monsoon over the SCS usually leads to less (more) precipitation over the mid-lower Yangtze Basin, and more (less) precipitation in North China.

(5) Sea-air fluxes have a close relationship with the monsoon activities. Before and after the onset of the southwest monsoon, with the abrupt variation of wind direction, wind speed, cloud cover, precipitation, humidity and sea surface condition, etc., the solar short-wave radiation, sea surface net radiation, latent heat flux and ocean heat net revenue and expenditure change acutely. Changes of sensible, latent heat, and momentum fluxes are subjected to different atmospheric elements. The sea surface sensible flux near the Xisha Islands during the period of the monsoon in 1998 is 7.8 W m^{-2} , and the latent flux is $110\text{-}130 \text{ W m}^{-2}$,

and the Bowen rate is 0.047-0.071, which are close to measurements in the other tropical regions. Ocean heat net budget change shows that before the onset of monsoon ocean energy is accumulated, during the onset of the monsoon ocean energy is released, and during the break period, there is a process of re-accumulation of ocean energy. With the weather and sea conditions, flux exchange coefficients (momentum exchange coefficient C_D , sensible heat exchange coefficient C_H , and latent heat exchange coefficient C_E) have greater changes, the relationship between them and the wind speed, sea-air temperature difference can be denoted by a polynomial or a linear relation.

(6) The sea temperature over the SCS in 1997-1998 is the highest in recent decades, the occurrence of the SCS warm event corresponded to the emergence of an ENSO event over the tropical eastern Pacific Ocean. Its appearance and weakening are closely linked with the change of the SCS monsoon. Likewise the circulation field over the SCS has an evident response to the ENSO event. For instance, the circulation structure can be reinforced during the El Niño event, while cyclonic eddy flows will decay in the northern SCS during the La Nina event. Furthermore, the importance of trapped Kelvin waves captured by boundary and westward propagating Rossby waves during the process of the sea-basin-scale circulation state over the SCS is revealed. An establishment mechanism of the monsoonal ocean circulation over the SCS is introduced. In addition, the SCS thermocline dynamics is explored, the SCS marine stratified structure is also studied, and a three-dimensional pattern of the SCS warm pool is presented.

(7) It is successful to simulate the monsoon fields and the seasonal variability and movement of rain belts and anomaly over the SCS and East Asian regions with regional climate models. China's major rainstorm events during the 1998 flood season were also successfully simulated. A coupled ocean-atmosphere regional climate model developed under the SCSMEX Project has a certain ability to reproduce the evolution of wind field of the East Asian monsoon and marine conditions.

Acknowledgments. South China Sea Monsoon

Experiment (SCSMEX) is the Key National Project of Climbing A during the period of 1996-2001, and supported strongly by the Ministry of Science and Technology, China Meteorological Administration, Chinese Academy of Sciences, and other departments. Many countries and regions as well as a lot of scientists involved in this project, and made important contribution to the successful implementation of the project.

Here we would like to express our deepest appreciation. Also we thank Prof. Chih-Pei Chang, Ka-Ming Lau, Johnson, Johnny Chung-Leung Chan, Jough-Tai Wang, Shou-Rong Wang, Qing-Chen Chao, Dun-Xin Hu, and Yong-Ping Zhao for their strong help and support. The great assistance rendered by Guangdong Meteorological Bureau is acknowledged. Finally the authors are much grateful to Ya-Fang Song, Qiang Xie, and Chun He for their help during the preparation of this paper.

REFERENCES

- Chang, C. P., and Chen G. T. J., 1995: Tropical circulation associated with southeast monsoon onset and westerly surge over the South China Sea. *Mon. Wea. Rev.*, **123**, 3254-3267.
- Chan, J. C. L., Wang Y. G., and Xu J. J., 2000: Dynamic and thermodynamic characteristics associated with the onset of the 1998 South China Sea summer monsoon. *J. Meteor. Soc. Japan*, **78**, 367-380.
- Chen Longxun, Zhu Q. G., Luo H. B., et al., 1991: *East Asian Monsoon*. China Meteorological Press, Beijing, 362 pp. (in Chinese)
- Chen Longxun and Wang Yuhui, 1998: Numerical experiment of impact of sea surface temperature in South China Sea and Warm Pool/West Pacific on East Asian summer monsoon. *Acta Meteor. Sinica*, **12**(2), 162-176.
- Chen Longxun and Zhu Congwen, 1998: Characteristics and mechanism analysis of SCS summer monsoon onset during SCSMEX in 1998. In: *Evolution of the South China Sea Monsoon and Its Interaction with the Ocean*. Ding Yihui and Li Chongyin, Eds. China Meteorological Press, Beijing, 13-17.
- Chen Longxun, Liu Hongqing, Wang Wen, et al., 1999: Preliminary study on the characteristics and mechanism of summer monsoon onset over South China Sea and region adjacent to it. *Acta Meteor. Sinica*,

- 57, 17-29. (in Chinese)
- Chen Longxun, Li Wei, and Zhao Ping, 2000: On the Process of Summer Monsoon Onset over East Asia. *Climate and Environmental Research*, **5**(4), 345-355. (in Chinese)
- Chen Yongli, Bai Xuezhi, and Zhao Yongping, 2000: A study on the relationships between the onset of the South China Sea summer monsoon and the anomalies of tropical ocean and atmospheric circulations. *Climatic and Environmental Research*, **5**, 388-399. (in Chinese)
- Chen Longxun, Zhu C. W., Wang W., et al., 2001: Analysis of the characteristics of 30-60 day low-frequency oscillation over Asia during 1998 SCSMEX. *Adv. Atmos. Sci.*, **18**(4), 624-628.
- Ding Yihui, 1993: *Study on the continuous exceptional heavy rain in the Changjiang-Huaihe River valley in 1991*. China Meteorological Press, Beijing, 47-130.
- Ding Y. H., 1992: Summer monsoon rainfalls in China. *J. Meteor. Soc. Japan*, **70**, 373-396.
- Ding, Y. H., and M. Murakami, 1994: *The Asian Monsoon*. China Meteorological Press, Beijing, 263 pp.
- Ding Y. H., 1994: *Monsoons over China*. Kluwer Academic Publishers, Dordrecht/ Boston/ London, 419 pp.
- Ding Yihui and Ma Henian, 1996: The present status and future of research of the East Asian monsoon. *The Recent Advances in Asian monsoon Research*. He Jinhai, Ed., China Meteorological Press, Beijing, 237 pp. (in Chinese)
- Ding Yihui and Li Chongyin, 1999: *Onset and Evolution of the South China Sea Monsoon and Its Interaction with the Ocean*. China Meteorological Press, Beijing, 423 pp.
- Ding Y. H. and Liu Y. J., 2001: Onset and the evolution of the summer monsoon over the South China Sea during SCSMEX field experiment in 1998. *J. Meteor. Soc. Japan*, **79**, 255-276.
- Ding Y. H., Li C. Y., and Liu Y. J., 2004: Overview of the South China Sea monsoon experiment. *Adv. Atmos. Sci.*, **21**(3), 343-360.
- Fong S., and Wan A. Y., 2001: *Climatological Atlas for Asian Summer Monsoon*. Macau Meteorological and Geophysical Bureau and Macau Foundation, 318 pp.
- Giorgi, F., M. R. Marinucci, and G. T. Bates, 1993a: Development of a second-generation regional climate model (RegCM2). Part I: Boundary-layer and radiative processes. *Mon. Wea. Rev.*, **121**, 2794-2813.
- Giorgi, F., M. R. Marinucci, and G. T. Bates, 1993b: Development of a second-generation regional climate model (RegCM2). Part II: Convective processes and assimilation of lateral boundary condition. *Mon. Wea. Rev.*, **121**, 2814-2832.
- Guo Qiyun and Wang Jiqin, 1981: Interannual variations of rain spell during predominant summer monsoon over China for recent thirty years. *Acta Geographica Sinica*, **36**(2), 187-195.
- He Jinhai, Xu Haiming, Zhou Bing, and Wang Lijuan, 2000: Large scale features of SCS summer monsoon onset and its possible mechanism. *Climate and Environmental Research*, **5**(4), 333-344. (in Chinese)
- He Jinhai, Ding Yihui, Gao Hui, and Xu Haiming, 2001: *Determination of the Date of South China Sea Monsoon Onset and Monsoon Index*. China Meteorological Press, Beijing, 123 pp. (in Chinese)
- He Jinhai, Xu Haiming, Wang Lijuan, et al., 2003: Climatic features of SCS summer monsoon onset and its possible mechanism. *Acta Meteor. Sinica*, **17** (Suppl.), 19-34.
- Huang Ronghui and Li Weijing, 1988: Influence of the heat source anomaly over the tropical western Pacific on the subtropical high over East Asia and its physical mechanism. *Chinese J. Atmos. Sci.*, Special Issue, 95-107. (in Chinese)
- Jiang Guorong, Sha Wenyu, and Yan Junyue, 2002: The analysis of the radiation features before and after South China Sea monsoon onset. *Journal of Tropical Meteorology*, **18**(1), 29-37.
- Johnson, R. H., and P. E. Ciesielski, 2002: Characteristics of the 1998 summer monsoon onset over the northern South China Sea. *J. Meteor. Soc. Japan*, **80**, 561-578.
- Lau, K. M., and S. Yang, 1997: Climatology and interannual variability of the Southeast Asian summer monsoon. *Adv. Atmos. Sci.*, **14**, 141-162.
- Lau, K. M., Ding Y. H., Wang J. T., et al., 2000: A report of the field operations and early results of the South China Sea Monsoon Experiment (SCSMEX). *Bull. Amer. Meteor. Soc.*, **81**, 1261-1270.
- Lau, K. M., and Weng H., 2002: Recurrent teleconnection patterns linking summertime precipitation variability over East Asia and North America. *J. Meteor. Soc. Japan*, **80**, 1129-1147.
- Li C., and Yanai, 1994: The onset and interannual variability of the Asian summer monsoon in relation to land-sea thermal contrast. *J. Climate*, **9**, 358-375.

- Li Chongyin and Zhang Liping, 1999: Summer monsoon activities in the South China Sea and its impacts. *Scientia Atmospherica Sinica*, **23**(3), 257-266. (in Chinese)
- Li C. Y., and Wu J. B., 2000: On the onset of the South China Sea summer monsoon in 1998. *Adv. Atmos. Sci.*, **17**(2), 193-204.
- Li C. Y., Long Z. X., and Zhang Q. Y., 2001: Strong/weak summer monsoon activity over the South China Sea and atmospheric intraseasonal oscillation. *Adv. Atmos. Sci.*, **18**, 1088-1099.
- Liu Hongqing and Chen Longxun, 1999: Numerical Experiment of the effect of SSTA on the SCS monsoon onset. In: *The Recent Advances in Asian monsoon mechanism Research*. Chen Longxun, Ding Yihui, M. Murakami et al. Eds., China Meteorological Press, Beijing, 268-280. (in Chinese)
- Liu Y. M., Chan J. C. L., Mao J. Y., et al., 2002: The role of Bay of Bengal convection in the onset of 1998 South China Sea summer monsoon. *Mon. Wea. Rev.*, **130**, 2731-2744.
- Liu Y. M. and Ding Y. H., 2003: Simulation of activity of the Asian summer monsoon and heavy rainfalls in China in 1998 with region climate model. *Acta Meteor. Sinica*, **17** (Suppl), 273-288.
- Matsumoto, J., 1997: Seasonal transition of summer rainy season over Indo-China and adjacent monsoon region. *Adv. Atmos. Sci.*, **14**, 231-245.
- Matsumoto, J., and T. Murakami, 2002: Seasonal migration of monsoon between the Northern and Southern Hemisphere as revealed from equatorially symmetric and asymmetric OLR data. *J. Meteor. Soc. Japan*, **80**, 419-437.
- Mu Mingquan and Li Chongyin, 2000: On the outbreak of South China Sea monsoon in 1998 and activity of atmospheric intraseasonal oscillation. *Climatic and Environmental Research*, **5**(4), 375-387. (in Chinese)
- Ninomiya, K., and T. Murakami, 1987: The early summer rainy season (Baiu) over Japan. In: *Monsoon Meteorology*. C. P. Chang and T. N. Krishnamurti, Eds., Oxford University Press, 93-121.
- Nitta, T., 1987: Convective activities in the tropical western Pacific and their impacts on the Northern Hemisphere summer circulation. *J. Meteor. Soc. Japan*, **65**, 373-390.
- Oh, J. H., W. T. Kwon, and S. B. Ryoo, 1997: Review of the researches on Changma and future observational study (KORMEX). *Adv. Atmos. Sci.*, **14**(2), 207-222.
- Qian Yongfu, Yan Hong, Wang Qianqian, et al., 1988: *Numerical Research on Topography Effect of Planetary Atmosphere*. Science Press, Beijing, 287 pp. (in Chinese)
- Qian, W. H., and D. K. Lee, 2000: Seasonal march of Asian summer monsoon. *Inter. J. Climatology*, **20**, 1371-1378.
- Qian Y. F., Zhang Y. Q., Zhang Y., et al., 2003: Response of China's summer monsoon climate to snow anomaly over the Tibetan Plateau. *Int. J. Climatol.*, **23**, 593-613.
- Qu S. H., Hu F., Li Y., et al., 2000: Some characteristics of air-sea exchange for the SCS summer monsoon during the SCSMEX in 1998. *Climatic and Environ. Res.*, **5**, 434-445.
- Ren, X. J., and Qian Y. F., 2005: A coupled regional air-sea model, its performance and climate drift in simulation of the east Asian summer monsoon in 1998. *Int. J. Climatol.*, **25** (5), 679-692.
- Tanaka, M., 1992: The ISO and onset and retreat dates of the summer monsoon over the east, southeast and western north Pacific region using GMS high cloud amount data. *J. Meteor. Soc. Japan*, **20**, 613-629.
- Tao, S. Y., and Chen L. X., 1987: A review of recent research on the East Asian summer monsoon in China. In: *Monsoon Meteorology*. C. -P. Chang and T. N. Krishnamurti, Eds., Oxford University Press, 60-92.
- Wu G. X., and Zhang Y. S., 1998: Tibetan Plateau forcing and the timing of the monsoon onset over South Asia and the South China Sea. *Mon. Wea. Rev.*, **126**, 913-927.
- Wang B., and Lin H., 2002: Rainy season of the Asian - Pacific summer monsoon. *J. Climate*, **15**, 386-398.
- Wu R. G., and Wang B., 2001: Multi-stage onset of the summer monsoon over the western North Pacific. *Climate Dynamics*, **17**, 277-289.
- Webster, P. J., V. O. Magana, T. N. Palmer, et al., 1998: Monsoon processes, predictability and the prospects for prediction. *J. Geophys. Res.*, **103**, 14451-14510.
- Wang B., and Fan Z., 1999: Choice of South Asian summer monsoon. *J. Climate*, **15**, 386-398.
- Wang B., and Ding Y. H., 1992: An overview of the Madden Julian Oscillation and its relation to monsoon and mid-latitude circulation. *Adv. Atmos. Sci.*, **9**, 93-111.
- Xie A., Mao J. Y., Song M. Y., et al., 1999: Impact of sea surface temperature and its variations on the onset of summer monsoon over the South China

- Sea. In: *The Recent Advances in Asian monsoon mechanism Research*. Chen Longxun, Ding Yihui, M. Murakami, et al., Eds., China Meteorological Press, Beijing, 205-218. (in Chinese)
- Yan Junyue, 1997: Climatological characteristics on the onset of the South China Sea southwest monsoon. *Acta Meteorologica Sinica*, **55**(2), 174-185.
- Yan J. Y., Yao H. D., Li J. L., et al., 2000: Characteristics of turbulence structure and flux transfer on the sea surface during the onset of SCS monsoon in 1998. *Climatic and Environmental Research*, **5**(4), 447-458.
- Yan J. Y., Yao H. D., Li J. L., et al., 2003: Air-sea heat exchange over the South China Sea under different weather conditions before and after southwest monsoon onset in 2000. *Acta Ocean. Sin.*, **22** (3), 369-383.
- Yeh Tu-Cheng, Dao Shih-Yen, and Li Mei-Tsun, 1958: The abrupt change of the atmospheric circulation during June and October. *Acta Meteorologica Sinica*, **29**(4), 249-263. (in Chinese)
- Zhao Z. C., Ding Y. H., Li X. D., et al., 1995: Evaluation of CGCM climate simulation in East Asian region. *Journal of Applied Meteorological Science*, **6**(Suppl.), 9-18.
- Zhu Baozhen, Ding Yihui, and Luo Huibang, 1990: A review of the atmospheric general circulation and monsoon in East Asia. *Acta Meteorologica Sinica*, **48**(1), 4-16.
- Zhu Kezhen, 1934: Southeast monsoon and precipitation over China. *Acta Geographica Sinica*, **1**, 1-28. (in Chinese)
- Zhu Qianguan and Xu Guoqiang, 2000: The features of LFP in South China with SCS LF summer monsoon activity in the summer of 1998. *Scientia Meteorologica Sinica*, **20**, 239-248. (in Chinese)